

1 **Identification of Source Faults of Large Earthquakes in the Turkey-Syria Border**
2 **Region Between AD 1000 and the Present, and their Relevance for the 2023 M_w 7.8**
3 **Pazarcık Earthquake**

4
5
6
7
8 **S. Carena¹, A. M. Friedrich¹, A. Verdecchia², B. Kahle^{1,3}, S. Rieger¹, and S. Kübler¹**

9
10 ¹Department of Earth and Environmental Sciences, Ludwig-Maximilians-Universität München,
11 Munich, Germany.

12 ²Institute for Geology, Mineralogy and Geophysics, Ruhr-Universität Bochum, Bochum,
13 Germany.

14 ³Department of Geological Sciences, University of Cape Town, South Africa.

15
16
17
18 Corresponding author: Sara Carena (scarena@iaag.geo.uni-muenchen.de)

19
20 **Key Points:**

- 21 • We identified the source faults of fourteen large earthquakes along the East Anatolian
22 and northern Dead Sea fault systems
- 23 • Maximum magnitude for the East Anatolian fault zone is approximately 8.2
- 24 • Continental transforms may be described as having a collective memory
- 25
26

27 Abstract

28 The February 6th, 2023, M_w 7.8 Pazarcık earthquake in the Turkey-Syria border region raises the
29 question of whether such a large earthquake could have been foreseen, as well as what is the
30 maximum possible magnitude (M_{max}) of earthquakes on the East Anatolian fault system and on
31 continental transform faults in general. To answer such questions, knowledge of past earthquakes
32 and of their causative faults is necessary. Here, we integrate data from historical seismology,
33 paleoseismology, archeoseismology, and remote sensing to identify the likely source faults of
34 fourteen $M_w \geq 7$ earthquakes between AD 1000 and the present in the region. We find that the
35 2023 Pazarcık earthquake could have been foreseen in terms of location (the East Anatolian
36 Fault) and timing (an earthquake along this fault was if anything overdue), but not magnitude.
37 We hypothesize that the maximum earthquake magnitude for the East Anatolian Fault is in fact
38 8.2, i.e. a single end-to-end rupture of the entire fault, and that the 2023 Pazarcık earthquake did
39 not reach M_{max} by a fortuitous combination of circumstances. We conclude that such unusually
40 large events are hard to model in terms of recurrence intervals, and that seismic hazard
41 assessment along continental transforms cannot be done on individual fault systems but must
42 include neighboring systems as well, because they are not kinematically independent at any time
43 scale.

45 Plain Language Summary

46 On February 6th, 2023, there was a magnitude 7.8 earthquake in the Turkey-Syria border region.
47 It surprised many people, including many Earth scientists, because of where it happened (on the
48 East Anatolian fault) and because of how large it was. People wondered whether it could have
49 been foreseen, and how large an earthquake on this fault can really be. To figure this out, we
50 looked at the history of earthquakes in the region in the last 1000 years. We used information
51 from historical seismology, paleoseismology, archeoseismology, and remote sensing to identify
52 the faults that caused fourteen earthquakes with magnitude 7 or greater in this region. We found
53 that the location (East Anatolian Fault) and timing (it was due any time) of the 2023 earthquake
54 were foreseeable, but not the magnitude. In fact, we believe that the maximum magnitude for the
55 East Anatolian Fault is 8.2, and that the 2023 earthquake was below this maximum just by
56 accident. It is hard to say how often such large events can happen, because many different things

57 need to align. We also believe that it is necessary to look at neighboring fault systems when
58 estimating seismic hazards, because they are all connected.

59

60 **1 Introduction**

61 The occurrence of the Feb. 6th 2023 M_w 7.8 Pazarcık earthquake surprised not only the
62 public, but also a large part of the geoscience community, due to the event size and location. This
63 earthquake ruptured ~310 km of the left-lateral East Anatolian Fault (EAF) between Antakya and
64 Çelikhan (Figure 1), which is ~55% of its length. It also ruptured through multiple segment
65 boundaries (Figure 2). The EAF had been, until February 2023, a “forgotten” plate boundary
66 fault, with the great majority of the more recent works mainly dealing with the North Anatolian
67 Fault (NAF) because of its proximity to Istanbul and of its higher level of seismic activity in the
68 past century. Even the most recent earthquake on the EAF, the Jan. 24th 2020 Elâziğ M_w 6.8
69 event, received surprisingly little attention. There are only 13 geoscience papers about this
70 earthquake listed in Web of Science. For comparison, the 1999 Düzce earthquake along the NAF
71 had 15 publications listed over the first 3 years after the event, even though publishing rates have
72 increased rapidly over time.

73 The EAF, however, has been documented as seismically very active in historical records,
74 with magnitudes above 7.0 inferred for multiple earthquakes around the EAF in the past 1000
75 years (e.g. Ambraseys, 1989, 2009; Guidoboni & Comastri, 2005; Sbeinati et al., 2005). For
76 most of these earthquakes, though, the specific source faults were not identified. Lack of
77 knowledge of source faults precludes the calculation of fault slip rates and recurrence times, and
78 the estimation of seismic hazards and M_{max} . It also precludes having a rigorous base for stress
79 and strain modeling and for studying dynamic rupture propagation.

80 Our goal is therefore to systematically identify the most likely source of each large ($M_w \geq$
81 7.0) earthquake along the East Anatolian and Dead Sea fault systems between Lake Hazar in the
82 north and Qalaat El Hosn, Syria, in the south (Figure 1) in the past ~1000 years, because these
83 earthquakes may have had a direct and significant influence on the timing, location, and size of
84 the 2023 M_w 7.8 Pazarcık earthquake. The more recent an earthquake is, the more likely it is to
85 have been the “last event” on its source fault, determining the last coseismic and postseismic

86 stress changes associated with the fault itself. Before AD 1000 the historical records are in any
87 case very fragmentary, making it impossible to associate most earthquakes with a specific fault.
88 By integrating historical records with paleoseismological ones in a tectonic context, we aim to
89 identify a set of reasonable fault / earthquake pairs and any plausible alternatives that can be used
90 for both modeling purposes and the identification of key field sites for further studies.

91

92 **2 Method and Results**

93 The identification by previous authors of source faults of historical earthquakes along the
94 EAF and northern Dead Sea Fault zone (DSF) is patchy. The typical case is, for example, when a
95 historical seismology work assigns an earthquake to a fault simply on the basis that it is a known
96 active fault in the general epicentral area. Often the source faults identified in this way are then
97 reported by later authors without any critical re-evaluation, even in those cases when the original
98 author had clearly stated that they were just doing a “best guess” approach with no additional
99 data. In most cases each work identifies one or two earthquake / source pairs, or identifies
100 multiple earthquakes, but all on the same fault. Unfortunately, identifying source faults in
101 isolation or without looking at all data available in both time and space is more likely to result in
102 mis-identification, the more so the older the earthquake is. We have therefore started from
103 published historical seismology works, re-evaluating each piece of information from different
104 authors about the same earthquake, and combining this with data from paleoseismology and
105 remote sensing (often more recent), following the approach suggested by Daëron et al. (2007) for
106 future studies on the DSF. We have not developed new methods, software, or collected field
107 data. Rather, we have carried out a comprehensive review of the information that already exists
108 and attempted to weed out inconsistencies and integrate information from different fields.
109 Finally, when reviewing information, we have done so for several earthquakes and faults
110 simultaneously, when these are (or could be) in the same sub-region.

111

112 2.1 Identification of source faults

113 In the case of the Turkey-Syria border region, several of the faults have been trenched, so
114 several events from the past 1000 years can be assigned to a specific fault with a reasonable

115 degree of confidence. In some cases, a couple of different options are equally plausible but,
116 overall, there is a limited combination of possible earthquake / source-fault pairs, because there
117 is only a limited number of faults in the area that are long enough to be credible source faults for
118 events of M_w 7 and above. We will start our analysis from those earthquakes for which there is
119 the most information available, and which may appear in one or more of the trenches, then move
120 to events which are less well-constrained. The order is not going to be strictly chronological,
121 because some of the older events are well-constrained, and some of the more recent ones are not.
122 We are going to start from the Amik basin area (Figure 1a), where the EAF and DSF come
123 together, and move first south and then north. The final list of earthquake / fault pairs that we
124 have determined to be the most likely can be found in Table 1, and the faults are shown in Figure
125 2b.

126 There are a few criteria that can be applied to the identification of the likely source fault
127 of a historical earthquake in the absence of dating of geological or archeological features: (1)
128 empirical relationships (e.g. Wells & Coppersmith, 1994) between earthquake size and fault
129 parameters (a large earthquake must have a long rupture, so determination of epicenter position
130 alone is not very meaningful), (2) the principle, based on Coulomb stress theory, that the same
131 fault segment or neighboring parallel faults (i.e. side-by-side) with the same kinematics are
132 highly unlikely to produce two large earthquakes within a few years or even decades of each
133 other, and (3) careful reading of earthquake effect descriptions, paying particular attention to
134 discussions by previous authors concerning reliability of sources. The latter is especially
135 important because it is not uncommon for mistakes to be spread from one earthquake catalog to
136 the next (or newly introduced) when information is accidentally left out, or two smaller
137 earthquakes are conflated into a larger one.

138 A new source of information that we have today, which was not available when all the
139 work on historical earthquakes in this region was being carried out, is the occurrence of the 2023
140 M_w 7.8 and 7.5 Turkey / Syria earthquakes (M_w from U.S. Geological Survey, 2023), which
141 allowed us for example to verify that the empirical relationship used by previous authors to
142 estimate magnitudes for historical earthquakes in this region is indeed appropriate (see Appendix
143 A for details). This earthquake is also invaluable in that it shows how fault segmentation can be
144 overcome to produce a very large earthquake, i.e. we should not fall into the trap of

145 automatically assuming a rupture cannot propagate past a bend or step when examining historical
146 earthquakes.

147 All the earthquakes that we consider are between AD 1000 and 2023, so “AD” is mostly
148 omitted throughout the paper. As no year has two earthquakes, throughout the text for simplicity
149 we only refer to the year of occurrence, omitting day and month. The precise date of each
150 earthquake (when known) is given in Table 1. Due to the fact that locality names and fault names
151 are very much relevant in this kind of work, in addition to the maps in Figure 1 we have supplied
152 details of naming (including rationale for specific choices) in Appendix B, and a full searchable
153 list of locality names with alternates as supplementary file ds04. Finally, as the number of place
154 names is quite large, we will not call a figure every time a place is mentioned: this paper should
155 be read with Figures 1 and 2 at hand at all times.

156

157 2.1.1 Amik basin and Dead Sea fault zone

158 We now apply the criteria described above to the earthquakes of 1872 and 1822. We start
159 with this pair because the 1822 earthquake was singled out by Ambraseys (1989) not only as one
160 of the largest earthquakes in the records, but also as one that took place in a region that - until
161 February 2023 - had very low seismicity.

162 Altunel et al. (2009) attributed the last event in their trenches at Demirköprü (Figure 3,
163 dated to between 1801 and 1940) to the 1872 earthquake based on their interpretation of
164 Ambraseys’s 1989 paper: “*Ambraseys (1989) reported that the 1822 earthquake took place in
165 the Karasu Valley located further north of the Amik Basin [...] it is therefore unlikely that the
166 event E1 can be related to the 1822 earthquake. Ambraseys (1989) also reports that the 1872
167 April 3 earthquake was responsible of heavy damage north and south of the former Amik Lake,
168 and in particular [...] around Qillig and Armenez. On the basis of both paleoseismic results and
169 historical accounts, we suggest that event E1 in trenches is related to the 1872 earthquake*”.
170 Ambraseys (1989), however, in the very next sentence to the one rephrased by Altunel et al.
171 (2009) also states (concerning the Qillig area and the 1872 earthquake): “*Here, it is said, the
172 earthquake split the ground in places and yellow sand filled the area, a description suggesting
173 widespread liquefaction*”. Liquefaction can happen at large distances from a fault surface rupture
174 (Ambraseys, 1988; Papathanassiou et al., 2005), so evidence of liquefaction is not evidence for

175 surface rupture at or near liquefaction location. In 2023, the M_w 7.8 earthquake caused
176 liquefaction in Kumlu (Quillig) and many other localities in the southern and eastern Amik
177 basin, even though the fault rupture was along the Amanos mountains front, and liquefaction was
178 reported also from localities up to at least 40 km away (Taftsoglou et al., 2023). Furthermore,
179 Ambraseys (1989) continues by writing, about the 1872 event: “*Also, between Batrakan and*
180 *Qaralu, the valley to the east of the hills is said to have dropped [...] and the ground was “rent”*
181 *all the way to Baghras, an allusion to faulting”*. The last three localities mentioned are at the foot
182 of the Amanos mountains, about 20 km apart along the mountain front, and 18 km west of the
183 trench site (Figures 1b and 3). Finally, the presumed location of the epicenter of the 1822 event
184 has no bearing on whether the source fault can or cannot pass through the trench, because the
185 epicenter of a historical earthquake simply indicates the center of the area of maximum damage
186 (i.e. the center of the “epicentral region”), but the source fault of the 1822 event must be at least
187 100 km long based on magnitude/length relationships, so it could easily go through the trench
188 site and have an epicenter elsewhere to the north. In fact, the isoseismals (lines of equal seismic
189 intensity) plot for the 1822 event of Ambraseys (1989) shows the maximum intensity as an
190 elongated region trending NNE, where the largest intensity isoseismal contains the trench
191 location.

192 If we consider all the evidence together, the most logical interpretation is that the likely
193 source of the 1872 event was the southernmost tip of the Amanos segment and, given the
194 widespread damage also reported all the way from Antakya to Samandağ, and in the mountain
195 villages on the Amanos mountains aligned parallel to this trend (Ambraseys, 1989), the faulting
196 likely extended in that direction towards the coast, possibly by linking with faults in the Antakya
197 fault zone (Figure 2b). Ambraseys (1989) plots isoseismals aligned with the southern termination
198 of the Amanos segment and centered on the Hatay graben. Ambraseys & Jackson (1998) stand
199 by the earlier interpretation of ground rupture for the 1872 event, as they report a 20 km rupture
200 length for this event in their catalog of “surface rupturing earthquakes”. This leaves the 1822
201 earthquake as the only possible rupture in the 1801–1940 age range to go through the trenches at
202 Demirköprü, because it is very unlikely that an unknown ground-rupturing earthquake (i.e. a
203 large one) would be missing from the records after 1800, especially one that would have strongly
204 affected such a historically important river crossing as the one at Demirköprü. If this is the case,

205 then also the event of compatible age (“after 1650 AD”) found by Akyüz et al. (2006) in the next
206 trench further south (Ziyaret, Figure 3) should be the 1822 earthquake.

207 The 1822 earthquake was a large event, as shown also by the fact that it was followed by
208 1.5 years of rather large aftershocks (Ambraseys, 1989, 2009), with the full aftershock sequence
209 terminating only after 30 months (Salamon, 2008). Ambraseys (1989) and Ambraseys & Jackson
210 (1998) estimated a magnitude of 7.5, which seems reasonable given the large area it affected and
211 the level of damage reported everywhere. Without explaining why, Sbeinati et al. (2005), though
212 also describing this as one of the most damaging earthquakes in the region, reduced the
213 magnitude to 7.0. A clue to the magnitude change could be the fact that several localities in
214 Turkey that had reported considerable damage (e.g. Gaziantep, and the towns west and northwest
215 of it) are not listed in their catalog, which would reduce the size of the affected area and thus the
216 magnitude. As there is no reason for the omission of these localities, we accept the determination
217 of M_w 7.5 of Ambraseys & Jackson (1998).

218 Different authors have placed the 1822 event either on the Amanos fault (e.g. Seyrek et
219 al., 2007), the Yesemek fault (e.g. Ambraseys & Melville, 1995; Duman & Emre, 2013), or the
220 St. Simeon fault (e.g. Karakhanian et al., 2008; Darawcheh et al., 2022). Even not considering
221 the likely presence of this earthquake in the trenches of Altunel et al. (2009) and Akyüz et al.
222 (2006) along the Orontes river valley, the Amanos fault is the least likely option: (1) the damage
223 pattern from the 1822 M_w 7.5 earthquake is shifted east and south compared to the damage
224 pattern of the 2023 M_w 7.8 earthquake (which definitely ruptured the Amanos segment, see
225 Figure 2b), (2) several foreshocks (the strongest preceding the mainshock by 30 minutes)
226 occurred in the region between Antakya, Latakia and Aleppo (Ambraseys, 1989, 2006),
227 suggesting that the main shock may have been triggered by the rupture of one of the many N-S
228 faults between the northern Ghab basin and the Amik basin, and (3) the epicenter estimated for
229 the 1822 event by both Ambraseys (1989) and Sbeinati et al. (2005) is located ~20 km east of the
230 Yesemek fault trace, albeit 60 km apart in latitude in either work (the location shift is also likely
231 due to the exclusion of the Turkish area around Gaziantep from the 2005 catalog). In addition,
232 Duman & Emre (2013) found no signs of a recent rupture along the Amanos fault in the Karasu
233 valley, whereas they claim that the Yesemek fault appears to show a fresher morphology, at least
234 in its northern segment (which is the one they checked in the field, on the Turkish side of the
235 border). Ambraseys (1989) identified the maximum intensity isoseismal as approximately

236 parallel to and slightly west of the Gaziantep-Kilis-Idlib trend. This is consistent with the
237 position and orientation of both the Yesemek fault and the northern segment of the St. Simeon
238 fault. Darawcheh et al. (2022) explicitly argue for the 1822 event to have originated on the St.
239 Simeon fault. These authors, however, identify as source fault what they call the “middle
240 segment” of the St. Simeon fault (actually, it is the southern segment, see Figure 4): this is a
241 mere 26 km long and a series of very short en-echelon segments (possibly a shear zone without a
242 throughgoing fault near the surface), i.e. too short to produce an earthquake of this magnitude.
243 Considering the parameters quoted by these authors (M_w 7.3 and a fault width of 15 km), an
244 average fault slip of about 10 m would be required, which is unrealistically large, as this is the
245 typical average slip value for M_w 8.0 (Wells & Coppersmith, 1994). A 26 km long fault would
246 normally produce roughly a M_w 6.7 earthquake, which does not match at all the historical
247 descriptions of destruction spread over a vast region. For the St. Simeon fault to be the source of
248 the 1822 earthquake, it would have had to rupture all the way from Afrin in the north to Sahen in
249 the south (i.e. rupturing part of the Apamea fault as well), breaking across the southern segment
250 too, which has a trend $\sim 30^\circ$ off from that of the two adjacent faults and, as pointed out above,
251 appears to be more a broad shear zone than a throughgoing fault. Also, if a surface rupture had
252 extended to the northeastern Ghab basin, the intensity at Maarret Missrin, Ram Hamdan, and
253 Binnish (all between 6 and 12 km from the southern St. Simeon fault segment) should have been
254 above the VII reported in Sbeinati et al. (2005). Finally, Karakhanian et al. (2008), while
255 speculating that the 1822 event may have occurred on the northern segment of the St. Simeon
256 fault (based on the epicenter location of Sbeinati et al., 2005), found no evidence of a recent
257 surface rupture on it, including at the site of the St. Simeon monastery, which they studied
258 extensively.

259 The most likely candidate for the 1822 earthquake thus appears to be the Yesemek fault
260 combined with part of the Qanaya-Babatorun fault, with a rupture extending from the Yesemek
261 fault northern segment for ~ 100 – 120 km south, past the Demirköprü bridge, to at least the
262 Ziyaret trench of Akyüz et al. (2006) (Figure 2b, 3). The next trench south (Yazlık) does not
263 have an event of compatible age, though it is possible that the event is simply not visible in the
264 trench because it followed a slightly different strand. In any case, a rupture from the latitude of
265 Islahiye in the north to south past Demirköprü and into the Orontes valley would explain the
266 especially strong damage in the Quseir region (which was also struck by numerous aftershocks,

267 reported by Ambraseys, 2009) and at the main crossings on the Orontes river (Demirköprü and
268 Jesr Al-Shughour), and the high damage region extending all the way to Sogce and Gaziantep in
269 the north.

270 The Yesemek fault has usually been mapped continuing south to the eastern edge of the
271 Amik basin (Duman & Emre, 2013) and possibly connecting to the Armanaz fault (Seyrek et al.,
272 2014). The Yesemek fault, however, splits into two branches south of 36.616643°N, both of
273 which are mapped as “active faults” in the active faults database of Zelenin et al. (2022). One
274 branch (the one called “Yesemek fault” or “East Hatay fault” by previous authors, see Appendix
275 B) continues with an almost N-S trend, whereas the other one turns southwest, following a series
276 of low hills, then disappears under the sediments of the Amik basin (Figure 2). We also know
277 that there is an active fault in the middle of the Amik basin. This fault is visible in the seismic
278 line of Perinçek & Çemen, 1990, and was re-interpreted by Seyrek et al. (2014), who reviewed
279 and synthesized existing subsurface data. Old geographic maps also show that the eastern
280 shoreline of the former Lake Amik and the eastern limit of the swamps north of the lake
281 followed this buried fault closely all the way to the eastern edge of the Karasu valley, meeting
282 the Yesemek fault there. It seems likely that this is the source fault of the 1822 earthquake
283 (Figure 2b), and that the fault interpreted by previous authors below the Amik basin is in fact the
284 Yesemek fault, which continues south and connects to the Qanaya-Babatorun fault near
285 Demirköprü.

286 The next pair of events that should be examined together is that of 1408 and 1404. The
287 1408 event has been identified most likely in all three trenches of Akyüz et al. (2006), who dated
288 event E1 “between 1310 and 1423” in the northernmost trench and “younger than 1019” in the
289 southernmost one. It could of course be either the 1404 or the 1408 earthquake, but as we will
290 see the 1404 earthquake is unlikely to have ruptured this far north. The maximum destruction
291 from the 1408 earthquake was along the trend from the Quseir region to Jesr Al-Shughour, with
292 significant damage also to Mahalibeh castle, and damage to Jableh and Latakia along the coast.
293 There is an open argument about the reported surface rupture, depending on the interpretation of
294 the Arabic word for the distance, given as either ~20 km (Ambraseys, 1989, 2009) or ~2 km
295 (Guidoboni & Comastri, 2005). The latter also claim there is no proof of damage in Antakya
296 (which in their case means magnitude reduction from the 6–7 of Ambraseys & Jackson, 1998, to
297 ~5.5), but Ambraseys (2009) reiterates that damage in Antakya is confirmed in reliable near-

298 contemporary Ottoman calendar sources, which Guidoboni & Comastri (2005) do not seem to be
299 aware of, as they do not mention them. Ambraseys (1989) puts forward two possibilities for the
300 source fault: either the Qanaya-Babatorun fault, or the Antakya fault zone, the latter based on the
301 fact that the damage extends towards the SW to the coast. A matter of contention here is again
302 the presumed surface rupture described in historical sources. Regardless of its length, the
303 location of the rupture is debated, because there is no agreement on where the village mentioned
304 in the ancient texts is located, near which the rupture may have terminated (the starting point was
305 in the Quseir region, i.e. between Antakya and the Orontes gorge, so not very specific either).
306 There are multiple spellings reported (Salthuam, Shalfuham, Salfhoum, Salthum), and this place
307 is identified by Ambraseys (1989, 2009) as Hisn Tell Kashfahan (in Jesr Al-Shughour), and by
308 Sbeinati et al. (2005) as Sfuhen (Sufuhon, on the eastern shoulder of the Ghab basin, Figure 1).
309 The latter seems to be too far east, and located on faults that are not connected to anything in the
310 Orontes gorge, but it could have been affected by a landslide triggered by the earthquake. So, if
311 Sufuhon is indeed the location mentioned, a landslide and a fault surface rupture must have
312 occurred at two different places. If Hisn Tell Kashfahan is the correct interpretation, then
313 landslide and fault surface rupture could have been at the same place. Either way, the earthquake
314 seems to have particularly affected one location that is clearly identifiable: the twin fortresses of
315 Shugr and Bekas (Shugur Qadim), located less than 2 km west of the Qanaya-Babatorun fault.
316 The key crossing on the Orontes of Jesr Al-Shughour, which sits on this fault trace, was also
317 destroyed. In Antakya, however, the damage does not appear to have been as extensive, so the
318 Qanaya-Babatorun fault seems a far more likely candidate than the Antakya fault zone, even
319 without considering the information from the trenches. The fault rupture most likely did not
320 extend north past the northernmost trench of Akyüz et al. (2006), because otherwise we would
321 expect reports of destruction at the Demirköprü historical “iron bridge”, as this crossing was a
322 vital one that had been in existence since well before 1000 AD. A ~40 km long rupture starting
323 at about the northern trench site and extending to Jesr Al-Shughour would produce a M_w 7.0
324 earthquake, in line with Ambraseys & Jackson (1998) estimate of a “6 to 7” magnitude. A 20 km
325 long rupture limited to the northern part of the fault appears too short to account for the
326 significant damage extending all the way to Mahalibeh castle, and a 2 km long rupture is

327 unrealistic, as the corresponding M_w 5.5. event would be too small to cause any damage along
328 the coast in Latakia and Jableh, which are 70 to 80 km away.

329 There is less information for the 1404 earthquake: Ambraseys (2009) and Guidoboni &
330 Comastri (2005) give essentially the same description from the same primary sources, and both
331 point out that one source wrongly adds some 1408 localities to the 1404 event description.
332 Sbeinati et al. (2005) used this source instead, apparently not realizing the problem, and
333 estimated M_w 7.4. Ambraseys & Barazangi (1989) estimated $M_w \geq 7.0$. This means the surface
334 rupture of the 1404 earthquake must have been at least 40 km long. From the damage
335 distribution, the source fault has to be somewhere around the Ghab basin. The Qanaya-
336 Babatorun fault is too far north to account for the significant damage to Marqab castle (on the
337 coast, 25 km south of Jableh), and for the intensity VII–VIII reported from Tripoli in Lebanon.
338 The Missyaf segment to the south is not a likely source, because the last event on this segment,
339 visible in the trench and in the displaced Roman aqueduct at Al-Harif, is the 1170 earthquake
340 (Meghraoui et al., 2003; Sbeinati et al., 2010). The two likely sources left are the Nusayriyah
341 fault at the western margin of the Ghab basin, and the Apamea fault at its eastern margin (Figure
342 2a). We believe the Nusayriyah fault to be the more likely source, based on two considerations.
343 The first is that the high damage reports are skewed towards the coast, pointing to a source on
344 the western rather than eastern Ghab basin, and the second is that an earthquake on this fault
345 segment in 1404 would be more effective in increasing the stress on the Qanaya-Babatorun fault,
346 which ruptured just 4 years later, than an earthquake on the Apamea fault. A final possibility,
347 which we cannot discount at this time, is that the earthquake resulted from the rupture of a fault
348 buried in the middle of the Ghab basin, as the presence of a fault here is known from geophysical
349 data (Rukieh et al., 2005).

350 The next significant event back in time in this area is the 1170 earthquake, which is well-
351 documented, with extensive descriptions by multiple authors (e.g. Ambraseys 1989, 2004, 2009;
352 Guidoboni et al. 2004b; Guidoboni & Comastri 2005). Guidoboni et al. (2004b) estimated M_w
353 7.7 +/- 0.22 and a fault length of 125 km. Ambraseys (2009) instead estimated M_w 7.3 +/- 0.3.
354 The source fault of this earthquakes has been identified by Meghraoui et al. (2003) as the
355 Missyaf segment of the DSF, with the 1170 event being the last rupture that occurred at the Al-
356 Harif aqueduct site. They suggested that the fault ruptured from Qalaat El Hosn to Apamea, a
357 distance of ~80 km. Meghraoui et al. (2003) and Sbeinati et al. (2010) established that the slip at

358 the aqueduct site in the 1170 event was 4 to 4.5 m. If this is maximum slip, it alone indicates M_w
359 7.3 to 7.4. This is compatible with the magnitude estimate of Ambraseys (2009), and reasonably
360 compatible with the damage distribution. The only outlier is the city of Aleppo as reported by
361 Guidoboni et al. (2004b), but Sbeinati et al. (2010) argue that these authors overestimated the
362 damage in Aleppo based on an erroneous interpretation of the chronicle by Ibn Al Athir. The
363 argument of Sbeinati et al. (2010) is reasonable, because the damage distribution is otherwise
364 very unusual, with a single intensity X locality (city of Aleppo) isolated and 200 km away from
365 the main intensity X region (Lebanon-Syria border southwest of Qalaat El Hosn). We therefore
366 agree with the source fault identification and rupture length of Meghraoui et al. (2003) and
367 Sbeinati et al. (2010).

368 In 1156–1157 there was a long earthquake sequence (an “earthquake storm”) in the
369 region between Homs and Aleppo, culminating with the largest event on Aug. 12, 1157
370 (Ambraseys, 2004, 2009). Guidoboni et al. (2004a) did not calculate magnitude or epicentral
371 area because of the difficulty in separating the numerous earthquakes in this period. Ambraseys
372 (2004, 2009) instead separated several of the larger events and calculated the magnitude of the
373 largest (7.2 +/- 0.3), and placed the location of the epicenter very close to the Missyaf fault near
374 Apamea. As mentioned above, the Missyaf fault last ruptured in 1170 through the Al-Harif site.
375 While it is possible that an older rupture followed a slightly different strand and did not pass
376 through the Al-Harif site, the Coulomb stress shadow due to an earthquake in 1157 would have
377 most likely precluded another large rupture of the same fault segment just 13 years later, because
378 such a short time is insufficient to significantly reduce the coseismic stress shadow from a $M_w >$
379 7 event. Based on the damage pattern, the St. Simeon fault is too far north, and the Nusayriyah
380 fault too far west. That leaves the Apamea fault and another unnamed fault of similar length just
381 10 km east of it (which here we name “Shaizar fault”, Figure 2a, 4). Because it appears that the
382 most damage was towards southeast (Hama, Salamiyah) and east (Ma’arat al-Nu’man, Kafar
383 Tab, Shaizar) of the Ghab basin, the Shaizar fault is a more likely source than the Apamea fault.
384 Sbeinati et al. (2005) put the epicenter on the Shaizar fault. Also, all of the 1156-1157 seismicity
385 was concentrated in the region between Aleppo and Hama east of this fault. The area is littered
386 with small faults (Figure 4), so it is conceivable that this is a case of small and moderate
387 earthquakes triggering one another, until one of them got close enough to trigger the largest of

388 these faults to rupture. The Apamea fault cannot, however, be excluded as a possible source
389 without further investigation.

390 We have previously argued that the St. Simeon fault is unlikely to be the source of the
391 1822 earthquake. There are two older earthquakes, however, which could have been produced by
392 this fault, in 1626 and 1138. The interpretation of this fault is controversial: some authors (e.g.
393 Westaway, 2004; Seyrek et al. 2014) claim that it belongs to an earlier tectonic phase and it is no
394 longer active. Others (Rukieh et al., 2005) instead consider it active, and some (Karakhanian et
395 al., 2008) have even found evidence of historical earthquake-related deformation along it, albeit
396 not an actual rupture of the main fault itself.

397 There is little information about the 1626 earthquake. Ambraseys only mentions it in his
398 2009 catalog and in Ambraseys & Finkel (1995), and Sbeinati et al. (2005) repeat the same
399 information, add one paragraph, and estimate a magnitude of 7.3. It appears to have been a fairly
400 damaging earthquake over a large area, but not much specific information has come to light.
401 Karakhanian et al. (2008) consider the St. Simeon fault a likely source, based on their
402 archeoseismological work on the St. Simeon monastery. A rupture of the northern segment of the
403 St. Simeon fault (~ 50 km long) could produce a M_w 7.2 earthquake, and in light of the reported
404 damage area (between Aleppo and Gaziantep) we believe that this fault is indeed a likely
405 candidate.

406 The authors who report extensively on the 1138 event are Ambraseys (2004, 2009),
407 Guidoboni et al. (2004a), and Guidoboni & Comastri (2005). Sbeinati et al. (2005) just give it a
408 brief mention, and this event does not even appear in the GEM historical catalog of Albini et al.
409 (2013). An estimated magnitude is only reported by Guidoboni & Comastri (2005) (M_e 6.0), and
410 apparently recalculated (without explanation, but from comparing the reported intensities it
411 seems it was done by just increasing the estimated intensity values) in the INGV catalog to M_e
412 7.5 (Guidoboni et al., 2018, 2019). Both Ambraseys (2004, 2009) and Guidoboni & Comastri
413 (2005) essentially give the same description concerning localities and damage, and date of the
414 earthquake. Guidoboni & Comastri (2005) also calculate the position of the epicenter on Mount
415 Quoros, which is just 15 km north of the termination of the St. Simeon fault. On the basis of
416 where the highest damage was, and where the earthquake was felt, the St. Simeon northern
417 straight segment, which could produce a M_w 7.2 earthquake, is a likely source. The estimated M_e

418 7.5 (INGV) is excessive, because it corresponds to a 110-120 km long rupture, which would
419 mean a rupture involving also the Apamea fault into the northern Ghab basin, with a very
420 different damage distribution. In fact, Guidoboni et al. (2014a) suggested that the entire 1138-
421 1139 sequence involved faults north-northeast of the Ghab basin, and not any of the faults that
422 bound the basin itself. Besides the northern St. Simeon fault, there are no other long enough
423 faults in the vicinity and in the proper position that would give the observed damage pattern. A
424 magnitude of 6.0 (Guidoboni & Comastri, 2005) on the other hand is too small, because such an
425 earthquake would have a radius with strong (VI) shaking of only about 20 – 30 km, and several
426 localities that reported significant damage (e.g. Tell Khalid, Tell Amar, Bizaah) are 60 to 100 km
427 away.

428

429 2.1.2 Karasu valley and East Anatolian fault zone

430 The pairing of earthquakes and source faults along the EAF north of the Karasu valley,
431 between Türkoğlu and Elâziğ, is somewhat more straightforward - albeit not entirely free of
432 controversy - because there are fewer active faults that need to be considered, and fewer post-AD
433 1000 large earthquakes. We have included one earthquake from 2020 with M_w 6.8 (Elâziğ
434 earthquake, Table 1), which is below our M_w 7.0 limit, because this is the only instrumental, 21st
435 century and pre-2023 earthquake to have occurred along the EAF and it delimits the 2023 M_w 7.8
436 rupture northeastern extent (Figure 2b), so it is included here for completeness. This earthquake
437 ruptured part of the Pütürge segment and did not appear to have a surface rupture (Çetin et al.,
438 2020), though ~0.5 m of shallow slip was identified by Pousse-Beltran et al. (2020).

439 The 2020 Elâziğ earthquake rupture is sandwiched between two other relatively recent
440 events: 1874 M_w 7.1 and 1893 M_w 7.2 +/- 0.1 (Ambraseys, 1989; Ambraseys & Jackson, 1998;
441 Ambraseys, 2009). Ambraseys (2009) reported that he confirmed in the field in 1967 the surface
442 rupture of the 1874 event, which involved the Palu segment between Palu and Pütürge
443 (Ambraseys & Melville, 1995). His evaluation of the historical documents indicates a ground
444 rupture about 45 km long, with 1–2 m uplift of the eastern block and unspecified left-lateral
445 strike-slip displacement.

446 The 1893 calculated epicenter (Ambraseys, 2009) is near Çelikhan, and Ambraseys &
447 Melville (1995) attributed the earthquake to the Erkenek segment. In the historical reports a

448 surface rupture is not described anywhere, but for an earthquake of this magnitude it would be in
449 the range of 45 to 70 km long. The rupture did not propagate south into the Pazarcık segment, as
450 there is no trace of it in the Balkar and Tevekkelli trenches (Figure 3) of Yönlü (2012). On the
451 basis of the isoseismal plot and epicenter location of Ambraseys (2009), the earthquake likely
452 ruptured most of the Erkenek segment, stopping ~ 20 km SW of Pütürge in the north, and near
453 Erkenek in the south (Figure 2b). A smaller (M_w 6.8) event in 1905 with a similar epicentral area
454 may have completed the rupture of this fault segment to the south, likely without a surface
455 rupture (it does not appear in the “surface rupturing” event list of Ambraseys & Jackson, 1998,
456 whereas the 1893 event does).

457 The last rupture of the Pazarcık segment prior to 2023 is well-documented, because
458 multiple trenches have been excavated across it (Yönlü, 2012). There are two historical large
459 events in the vicinity of this segment that we need to consider: one in 1114, and the other in
460 1513/1514. The oldest of the two is the better documented one, even though it appears as two
461 separate events in different catalogs. This earthquake is discussed in detail by Ambraseys (2004),
462 who reported it as having happened on Nov. 29th 1114. Ambraseys (2004, 2009) went to some
463 length to explain why there are differences in reported dates, and concluded that Nov. 29th 1114
464 is the correct one. This earthquake was assigned a magnitude of “large” (i.e. 7.0 to 7.8) by
465 Ambraseys & Jackson (1998), and 6.9 +/- 0.3 by Ambraseys (2009). Guidoboni & Comastri
466 (2005) instead split the event in two, on different dates and locations (Nov. 13th 1114 Maraş, M_e
467 6.3, and Nov. 29^h 1115 Misis, M_e 6.4). Ambraseys (2009) states that it is unclear why they split
468 the event and that in 1114 there were several other strong shocks in the region before the one on
469 Nov. 29th, but the latter was by far the largest one in the series. One of the two shocks of
470 Guidoboni & Comastri (2005) (Nov. 13th 1114) is in fact listed as a separate foreshock by
471 Ambraseys (2009). Ambraseys (2009) also reported that some sources mention an earthquake in
472 this region in 1115, and this was likely a strong aftershock. Sbeinati et al. (2005) also split the
473 earthquake into two events that have same description and same general area, but different
474 magnitudes (7.4 and 7.7), both of them in Nov. 1114 (no day given, they just state within the
475 same entry that this event could be two earthquakes). Here the confusion is increased by the fact
476 that in the parametric list the authors supply two distinct epicenters and magnitudes, but an
477 identical list of affected localities and intensities, so it is unclear how they were able to compute
478 different epicenters and magnitudes. One of the two (M_w 7.4, with epicenter near Şanlıurfa, east

479 of the Euphrates valley) has been included in the GEM catalog of Albini et al. (2013), whereas
480 the second 1114 earthquake in the GEM catalog has been taken from Ambraseys (2009), again a
481 choice without apparent explanation. There is no trace in Ambraseys's papers and in his 2009
482 catalog of any events in 1114 that affected mainly the region around Şanlıurfa: the two significant
483 "foreshocks" mentioned were in the Iskenderun bay region. In fact even the 1115 event of
484 Guidoboni & Comastri (2005) is located between the Iskenderun bay region and Maraş.
485 Ambraseys (2009) stressed how the descriptions of this earthquake are split between "western"
486 and "eastern" primary sources: this could explain the tendency of recent authors to produce two
487 main shocks for the same event. Finally, the parametric catalog of Kondorskaya & Ulomov
488 (1999) lists for this event M_w 8.1, and the event epicenter location (a single one for 1114, but on
489 August 10, the date for which Ambraseys 2004 reports a strong shock possibly offshore
490 Iskenderun) is placed between the locations of Ambraseys (2004) and Sbeinati et al. (2005).
491 Considering that M_w 8.1 is close to the magnitude expected for a complete rupture of the entire
492 EAF, this catalog clearly overestimates the size. In summary, for the earthquake of November
493 1114 the works of Ambraseys are more reliable, because there is a justification for each
494 determination made (date, location, magnitude) and clear exclusion of other possibilities. We
495 therefore chose to accept the information given in the latest work (Ambraseys, 2009) for the
496 parameters of this earthquake, which place it somewhere along the Pazarcık segment of the EAF.
497 Yönlü (2012) found a rupture compatible with a 1114 event in three trenches along the EAF
498 (Nacar, and Balkar 1 and 2, Figure 3): there E1 has been dated to before 1153 and after 677, and
499 this rupture is not present in their Tevekkelli trench, 35 km further southwest along the fault.
500 From the paleoseismological findings a surface rupture length of 60 km has been estimated
501 (Gürboğa, & Gökçe, 2019), placing the 1114 earthquake on the northern two-thirds of the
502 Pazarcık segment with M_w of at least 7.1. This is compatible with the size estimated by
503 Ambraseys (2009), but not with the estimates of Guidoboni & Comastri (2005), Sbeinati et al.
504 (2005), and Kondorskaya & Ulomov (1999), further confirming that the earthquake location of
505 Ambraseys (2009) is most likely the correct one. This event does not appear in any form in the
506 trenches and core from Lake Hazar (Hazar Gölü, Figure 3; Çetin et al., 2003; Hubert-Ferrari et
507 al., 2020), so probably its magnitude was not larger than the estimated 7.1, even though

508 Ambraseys & Jackson (1998) considered it a possible candidate for a truly large earthquake (i.e.
509 of magnitude closer to 7.8 than to 7.0).

510 The only authors to report on the 1513 earthquake in recent papers and catalogs are
511 Ambraseys (1989, 2009), and Ambraseys & Finkel (1995). The exact year (late 1513 or early
512 1514) is also debatable. There is very little specific information about the earthquake, but
513 Ambraseys (1989) claims that, given the size of the area over which it was felt (even in the
514 absence of specific damage descriptions), the magnitude was significant (≥ 7.4). Apparently, the
515 regions of Tarsus, Adana, Malatya, and around Haçın were strongly affected. His calculated
516 epicenter location puts the earthquake within 30 km of the EAF (~ 30 km ENE of Türkoğlu),
517 while the uncertainty radius is ~ 50 km, so a location of the event on the EAF is entirely
518 plausible. The Tevekkelli trench of Yönlü (2012) contains a rupture for E1 dated to between
519 1440 and 1630, which is compatible with an earthquake in 1513/1514. In the three trenches
520 further northeast along the EAF (Nacar, and Balkar 1 and 2) instead E1 is dated to between 677
521 and 1153, so the 1513 event is not visible. The closest trench to Tevekkelli (the Nacar trench) is
522 35 km northeast of it, so the rupture should have stopped before reaching this point, which means
523 it is unlikely for the 1513 earthquake to be the penultimate event (E2) tentatively identified by
524 Çetin et. (2003) in one of their Lake Hazar trenches (they date E2 to AD 1393 – 1464, but claim
525 that, because of dating uncertainties, it could be the 1513 earthquake). In the catalog of trenches
526 in Turkey (Gürboğa & Gökçe, 2019), the 1513 rupture is estimated as 40 km long. This is barely
527 the equivalent of a rupture of the Pazarcık segment between about 10 km southwest of the Nacar
528 trench and Türkoğlu. A 40 km rupture however would not produce an earthquake above M_w 7.0.
529 A M_w 7.4 earthquake requires a 80 km long rupture. That can be done by the rupture extending
530 from south of the Nacar trench to Islahiye, i.e. rupturing the southern part of the Pazarcık
531 segment and then the Nurdağı segment of the Amanos fault to the next bend south near Islahiye
532 (Figure 2b). This would be more in line with an event that must have produced considerable

533 damage to the region of Adana and Tarsus. A rupture stopping at Türkoğlu and a M_w of 7 would
534 not have been sufficient, this region being 180 km away.

535

536 **3 Discussion: timing, location, and size of the 2023 M_w 7.8 Pazarcık earthquake**

537 3.1 Fault segmentation, rupture length, and earthquake size

538 In the Karasu valley, the central and southern Amanos fault (Hassa segment and most of
539 the Kirikhan segment, Figure 2a) does not appear to have ruptured in a large earthquake at any
540 time from at least AD 1000 to 2023 between Baghras and Islahiye, a fault length of ~ 70 km
541 (Figure 2b, 5a). This could partly explain the unusually large size of the 2023 M_w 7.8 earthquake:
542 the central and southern Amanos segments, which are separated from the Nurdağı segment by a
543 releasing bend near Islahiye, and from each other by a restraining bend near Demrek (Duman &
544 Emre, 2013), were stressed enough that the bends not only were insufficient to stop a multi-
545 segment rupture, but may have contributed to it. In fact, it appears that the Demrek restraining
546 bend was a region of higher slip from the surface to ~ 10 km depth (Barbot et al., 2003). Recent
547 studies on large thrust earthquakes (e.g. 2008 M_w 7.9 Wenchuan earthquake, Wan et al. 2017)
548 suggest that stepovers along faults, and especially restraining stepovers, build up slip deficit over
549 time merely because of their geometric complexity, and when they finally rupture they provide
550 energy for the rupture to propagate even further, which it seems is what happened on the
551 Amanos fault. Thus, the most likely reason we have not seen such large ruptures before on the
552 EAF is not because “fault segmentation” or “fault maturity” determine the maximum length of
553 rupture in plate boundary faults, but rather because they are infrequent and, therefore, not
554 captured by the comparatively short and incomplete earthquake history we have for the region.
555 For a M_w 7.8 earthquake to happen, which, let’s not forget, ruptured over half of the EAF at
556 once, we need a rather specific set of circumstances that are hard to quantify in the absence of
557 data.

558 Prior to 2023, there was considerable disagreement over the maximum size of
559 earthquakes on the EAF. For example, Hubert-Ferrari et al. (2020), on the basis of the historical
560 seismicity reports, assumed that magnitude 7.0 and above is likely, whereas some studies based
561 on the instrumental record alone considered M_{\max} for the EAF to be limited to M_w 6.8 (e.g.
562 Bayrak et al., 2015), while yet others proposed a range from M_w 6.7 to 7.4 depending on the

563 segment considered (e.g. Gülerce et al. 2017; Güvercin et al., 2022), with up to M_w 7.7 when
564 some segment combinations are explored in models (Gülerce et al., 2017). A good estimate of
565 M_{max} , however, is crucial for seismic hazard assessments. In the case of faults like the EAF,
566 which have no large instrumentally-recorded events, knowledge about M_{max} , recurrence
567 intervals, and rupture length can only come from a combination of historical records,
568 paleoseismological studies, geological analysis in tectonic context, and comparisons with similar
569 faults. Based on the information available at the time, the 2023 M_w 7.8 earthquake could have
570 been foreseen in terms of location and timing (an earthquake on the southern EAF was due any
571 time, this fault being a clearly active one currently in -what should have been an alarmingly-
572 quiescent period), but not in size, because the largest confirmed earthquake in historical catalogs
573 since AD 1000 for the region reached M_w 7.5 at most, with the majority of earthquakes being M_w
574 7 to 7.2 (Table 1). Besides, the source fault of the M_w 7.5 earthquake in 1822 is not technically
575 even part of the EAF system. Looking further back in time (before AD 1000) would not have
576 increased the number of truly large earthquakes, as such events are even harder to interpret the
577 older the records are: there are none listed for this area by Ambraseys & Jackson (1998), but that
578 does not mean none happened, just that they may not have been recognized or recorded. With no
579 earthquakes of comparable size in either instrumental or historic catalogs, we cannot calculate an
580 observed recurrence interval for $M_w \geq 7.8$ on the EAF, and are left with estimates based on
581 geodetic rates or longer-term average geological displacement rates (e.g. Friedrich et al., 2003).
582 This is only half the problem though: without a $M_w \geq 7.8$ in the records, the possibility that such
583 an earthquake would occur on the EAF was not seriously considered in seismic hazard
584 calculations for the region by most authors. We propose that for the EAF M_{max} is actually ~ 8.2 ,
585 i.e. a complete rupture from the Karlıova triple junction to the Amik triple junction (Figure 1d),
586 and that all continental strike-slip plate boundary faults should be treated as having the same
587 end-to-end rupture potential, unless proven otherwise. In this context, M_{max} is reached in
588 “superevents” that are infrequent and most likely highly non-periodic, especially for non-isolated
589 plate boundary faults such as the EAF-DSF system (contrast with the Alpine Fault, NZ,
590 Berryman et al., 2012) and thus not captured by even such a comparatively long historical record
591 as we have for Anatolia. The 2023 M_w 7.8 earthquake did not reach M_{max} only by a fortuitous
592 combination of circumstances. It appears that the combined effect of the larger stepover between
593 the Erkenek and Pütürge segments and the coseismic Coulomb stress shadow from the 2020

594 Elâziğ event on the latter was enough to stop the 2023 rupture from dynamically propagating
595 further to the northeast. Understanding how and in what measure fault geometry and prior stress
596 history each contributed to stopping the rupture will need careful modeling. The 2023 M_w 7.8
597 earthquake stands as a warning that continental transforms can fully rupture just as subduction
598 thrusts can (see McCaffrey, 2008), in infrequent but devastating earthquakes.

599

600 3.2 Fault interactions, cascades, cycles, supercycles, and collective memory

601 The reason for the behavior of the EAF is multifaceted. First of all, there is the
602 intertwined kinematics of the three plate boundary fault systems: EAF, DSF, and NAF (Figure
603 1d). Hubert-Ferrari et al. (2003) pointed out that the EAF and NAF cannot move simultaneously,
604 and that in the historical records since AD 100 the number of damaging earthquakes on each
605 fault reflects this, with peak seismic activity switching from one fault zone to the other every few
606 hundred years. For the DSF, Khair et al. (2000) also observe a switching between activity and
607 quiescence, with quiescent periods of 450–700 years interrupted by active periods of 50–150
608 years in the past two millennia. These are examples of supercycles (e.g. Philibosian and
609 Meltzner, 2020; Salditch et al., 2020).

610 Whereas plate-boundary-scale kinematics and variations in long-term strain accumulation
611 may control the acceleration and the turning-on-and-off of each fault zone on the million-year to
612 the millennial scale (i.e. supercycles and clusters; see also Friedrich et al., 2003; Bennett et al.,
613 2004, Lefevre et al., 2018), within each period of high activity the seismic behavior is likely
614 controlled by coseismic and postseismic Coulomb stress changes (King et al. 1994). The latter is
615 indicated by the clustering of earthquakes within relatively short time periods, and by the
616 propagation of ruptures in systematic fashion along some faults: for example, the classic NAF
617 behavior of east-to-west sequential ruptures (e.g. Barka, 1996; Stein et al., 1997; Hubert-Ferrari
618 et al., 2000, 2003), but also the behavior observed on the EAF, where a series of ruptures can
619 start at both ends of the fault system and move towards the center (Hubert-Ferrari et al., 2003).
620 Another potential example of this behavior is the rupture cascade (Philibosian and Meltzner
621 2021) of the 12th century (cf. Figure 7.2 in Marco and Klinger, 2014) along the EAF and DSF
622 systems in a southerly direction. The 1114 event occurred along the Parzarcık segment of the
623 EAF (Figure 2b). Then, the DSF ruptured several times as documented by the 1138, 1157, and

624 1170 events (Figure 2b and 5), and the 1202 event in Lebanon (South Yammouneh segment,
625 DSF, Daëron et al., 2007). After the 12th century cascade, both fault zones appear to have
626 ruptured irregularly. As a result, the time since the last major ($M_w > 7$) event varies along strike
627 of the fault zones. For the EAF, the times since the last rupture events are 130 years (Erkenek
628 segment), 500 years, 900 years, and over 1000 years for the Amanos segment (Figure 5a). These
629 seismic gaps are not due to a lack of data, but rather are an expression of the natural earthquake
630 behavior in active fault zones. Thus, for fault segments where a seismic gap exists, the maximum
631 possible earthquake magnitude (M_{max}) may be severely underestimated unless seismic activity
632 from the entire fault system going back several thousand years is considered. For example,
633 seismic hazard modeling conducted solely based on instrumental seismic records prior to
634 February 6th, 2023, treated such segments as inactive and underestimated M_{max} and the seismic
635 hazard (e.g. Bayrak et al., 2015). The February 6th, 2023 Pazarcık earthquake filled in the large
636 seismic gaps in the Amanos segment and several other seismic gaps along strike (Figure 5b). If
637 the same type of hazard modeling would be conducted after February 6th, the Amanos segment
638 will appear as active and be included, thereby likely overestimating its hazards in the near future.

639 Similar seismic gaps also exist along the DSF, some lasting for 200 years, while others
640 lasting for 620 years, and over 850 years (Figure 5c). These seismic gaps will grow, close, and
641 reopen repeatedly (Figure 5d) as long as strain accumulates across this active plate boundary,
642 and when a seismic gap exists without a recent stress shadow, the hazard is high. The
643 identification of seismically inactive but geodetically active regions along active fault zones is,
644 therefore, an important area of focus for future research and seismic hazard assessment, but
645 additional information is required to accurately forecast earthquake potential.

646 There is also an important role played by local fault configuration, in this case especially
647 the branching of EAF and DSF. The two systems are not independent, even on short time scales.
648 These two fault zones overlap, with faults from both zones running parallel to one another and
649 having very similar kinematics in a strip just a few tens of km wide. Thus, in the Karasu valley
650 and Amik basin, depending on exactly which fault ruptures where, there can be either Coulomb
651 stress loading or shadowing of neighboring faults belonging to either fault zone. For example,
652 the northwestern DSF strands (Qanaya-Babatorun and Nusayriyah faults) have likely been
653 loaded coseismically by the 2023 M_w 7.8 earthquake, simply on the basis of their relative
654 position, geometry, and kinematics. On the other hand, the Amanos segment and the Yesemek

655 fault in the Karasu valley have the same configuration as the southern San Andreas/San Jacinto
656 fault pair in California: two closely-spaced (15 to 30 km) subparallel faults with the same strike-
657 slip kinematics. This is a situation where the faults are effectively coupled: a large rupture on one
658 fault would cause a significant coseismic Coulomb stress drop on the other, delaying the next
659 rupture (Carena et al., 2004). The 1822 earthquake on the Yesemek fault therefore must have
660 delayed the occurrence of the next earthquake on the central-southern Amanos fault, which at
661 that point had not seen a rupture for at least 800 years, and the end of this delay just happened to
662 coincide with a fortuitous rupture propagation from a minor fault in the Narlı fault zone (Figure
663 2a) to the main branch of the EAF (Rosakis et al., 2023; U.S. Geological Survey, 2023), at a
664 position on the Pazarcık segment of the EAF that also had not seen a rupture in 900 years. This
665 was a classic “domino effect” with all tiles in the right place at the right time. We are thus left
666 with a question that can be answered only with further investigations: how often can the tiles line
667 up in this specific order? It is not a trivial problem: not only a specific set of circumstances can
668 lead to an unusually large event, but also activity on one fault system could control the timing of
669 the next supercycle of its immediate neighbor. It means that calculation of earthquake probability
670 cannot be restricted to one fault, or even one fault system: in the case of continental plate
671 boundary faults, it also needs to include the neighboring fault systems. Plate boundary faults may
672 not just have a “long term memory” (Salditch et al., 2020), but also a “collective memory” due to
673 their coupling by geometric characteristics of the fault systems and stress transfer patterns
674 between them, which would call for earthquake probability calculation at much larger scales than
675 is generally considered.

676

677 **4 Conclusions**

678 Within the limitations of the information available, we were able to define the most likely
679 pairs of historical earthquakes and their source fault segments along the EAF and northern DSF
680 since AD 1000. We tried to provide a comprehensive explanation for the choices we made in
681 each case, so that the data we produced can be evaluated for level of uncertainty, and used by

682 others either for earthquake modeling, or to identify locations that should be targeted in future
683 paleoseismological studies.

684 By considering the previous rupture history and geometric configuration of the faults
685 involved, we were able to address the reasons why the 2023 M_w 7.8 earthquake occurred on the
686 southern half of the EAF, why the conditions were right for it to occur now, and why it was
687 unusually large compared to previous events in the region. The main branch of the EAF had a
688 seismic gap of at least 1000 years at its southern end. A major rupture here was likely delayed by
689 the 1822 earthquake on the Yesemek fault (which could explain why the 1872 rupture did not
690 propagate northwards), but the stress shadow from this dissipated in about a century, paving the
691 way for any rupture to either initiate on or propagate unimpeded into the southern Amanos
692 segment. Based on the historical seismic records of the region, the 2023 M_w 7.8 Pazarcık
693 earthquake was foreseeable in space and time, but not in size. M_{max} for the EAF is likely ~ 8.2 ,
694 with the limit rupture length being the distance between the two triple junctions that delimit it.
695 The 2023 earthquake may not have reached M_{max} simply by a fortuitous combination of factors:
696 if the 2020 Elâziğ earthquake had not happened where and when it did, would the 2023 rupture
697 have continued propagating towards the northeast? This is a question that could be answered by
698 combining Coulomb stress models and dynamic rupture models. If nothing else, what we have
699 learned from the 2023 M_w 7.8 Pazarcık earthquake is that segmentation of continental transform
700 faults is not relevant for calculating M_{max} , because some earthquakes can jump across segment
701 boundaries. Such earthquakes are so infrequent, however, that they are difficult to study, and
702 therefore hard to foresee.

703

704 **Acknowledgments**

705

706 **Open Research**

707 All the data and software we used have been published or made available by the authors and
708 entities cited in the references list: digital elevation models (ESA, 2023, <https://doi.org/10.5270/ESA-c5d3d65>, Tozer et al. , 2019, <https://doi.org/10.1029/2019EA000658>), active fault database (Zelenin
709 et al. 2022, <https://doi.org/10.5194/essd-14-4489-2022>), pixel-tracking data (ForM@Ter – EOST ,
710 2023, doi:10.25577/EWT8-KY06, Ou et al. 2023,

712 <https://dx.doi.org/10.5285/df93e92a3adc46b9a5c4bd3a547cd242>), active fault database
 713 (<https://doi.org/10.5194/essd-14-4489-2022>), preliminary surface rupture mapping (Reitman et al.,
 714 2023, <https://doi.org/10.5066/P98517U2>), and texture-shading program (Brown, 2014;
 715 <https://app.box.com/v/textureshading>). The file with the electronic version of the ruptures listed in
 716 Table 1 and shown in Figure 2b is part of the supplementary material. We have also included in the
 717 supplement the uninterpreted base images of Figures 2b and 4.

718

719 **References**

- 720 Akyüz, H. S., Altunel, E., Karabacak, V., & Yalçiner, Ç., (2006), Historical earthquake activity
 721 of the northern part of the Dead Sea Fault Zone, southern Turkey. *Tectonophysics*, 426
 722 (1-2), 281–293. <https://doi.org/10.1016/j.tecto.2006.08.005>
- 723 Albini, P., Musson, R. M. W., Gomez Capera, A. A., Locati, M., Rovida, A., Stucchi, M., &
 724 Viganò, D. D., (2013), Global Historical Earthquake Archive and Catalogue (1000-1903),
 725 GEM Technical Report 2013-01 V1.0.0, 202pp., GEM Foundation, Pavia, Italy, doi:
 726 10.13117/GEM.GEGD.TR2013.01.
- 727 Altunel, E., Meghraoui, M., Karabacak, V., Akyüz, S. H., Ferry, M., Yalçiner, Ç., et al., (2009),
 728 Archaeological sites (Tell and Road) offset by the Dead Sea Fault in the Amik Basin,
 729 Southern Turkey. *Geophysical Journal International*, 179, 1313–1329. doi:
 730 10.1111/j.1365-246X.2009.04388.x
- 731 Ambraseys, N.N., (1988), Engineering seismology. *Earthquake Engineering and Structural*
 732 *Dynamics* 17, 1–105. <https://doi.org/10.1002/eqe.4290170101>
- 733 Ambraseys, N. N., (1989), Temporary seismic quiescence: SE Turkey. *Geophysical Journal*
 734 *International*, 96(2), 311–331. <https://doi.org/10.1111/j.1365-246X.1989.tb04453.x>
- 735 Ambraseys, N. N., (2004), The 12th century seismic paroxysm in the Middle East: a historical
 736 perspective. *Annals of Geophysics*, 47, 733–758. DOI: 10.4401/ag-3303
- 737 Ambraseys, N., (2009), Earthquakes in the Mediterranean and the Middle East: A
 738 multidisciplinary study of seismicity up to 1900. Cambridge University Press, New York,
 739 947 pp. <https://doi.org/10.1017/CBO9781139195430>
- 740 Ambraseys, N. N., & Barazangi, M., (1989), The 1759 earthquake in the Bekaa Valley:
 741 Implications for earthquake hazard assessment in the Eastern Mediterranean region.
 742 *Journal of Geophysical Research: Solid Earth*, 94, 4007–4013.
 743 <https://doi.org/10.1029/JB094iB04p04007>

- 744 Ambraseys, N. N., & Finkel, C., (1987), Seismicity of Turkey and neighbouring regions 1899-
745 1915. *Annales Geophysicae, Series B*, 5(6), 701–725.
- 746 Ambraseys, N. N., & Finkel, C., (1995), The seismicity of Turkey and adjacent areas: A
747 historical review, 1500–1800. Eren, Istanbul, 1995, 240 pp.
- 748 Ambraseys, N. N. & Jackson, J. A., (1998), Faulting associated with historical and recent
749 earthquakes in the Eastern Mediterranean region. *Geophysical Journal International*,
750 133, 390–406. <https://doi.org/10.1046/j.1365-246X.1998.00508.x>
- 751 Ambraseys, N. N. & Melville, C. P., (1995), Historical evidence of faulting in Eastern Anatolia
752 and Northern Syria. *Annali di Geofisica*, 38, 337–343. DOI: 10.4401/ag-4110
- 753 Barbot, S., Luo, H., Wang, T., Hamiel, Y., Piatibratova, O., et al., (2023), Slip distribution of the
754 February 6, 2023 M_w 7.8 and M_w 7.6, Kahramanmaraş, Turkey earthquake sequence in
755 the East Anatolian Fault Zone. *Seismica*, 2.3. doi:10.26443/seismica.v2i3.502
- 756 Bayrak, E., Yılmaz, Ş., Softa, M., Türker, T., & Bayrak, Y., (2015), Earthquake hazard analysis
757 for East Anatolian fault zone, Turkey. *Natural Hazards*, 76, 1063–1077.
758 <https://doi.org/10.1007/s11069-014-1541-5>
- 759 Bennett, R. A., Friedrich, A. M., & Furlong, K. P., (2004), Codependent histories of the San
760 Andreas and San Jacinto fault zones from inversion of fault displacement rates. *Geology*,
761 32(11), 961–964. <https://doi.org/10.1130/G20806.1>
- 762 Barka, A., (1996), Slip distribution along the North Anatolian fault associated with the large
763 earthquakes of the period 1939 to 1967. *Bulletin of the Seismological Society of America*,
764 86(5), 1238–1254. <https://doi.org/10.1785/BSSA0860051238>
- 765 Berryman, K. R., Cochran, U. A., Clark, K. J., Biasi, G. P., Langridge, R. M., & Villamor, P.,
766 (2012), Major earthquakes occur regularly on an isolated plate boundary fault. *Science*,
767 336(6089), 1690–1693. DOI: 10.1126/science.1218959
- 768 Brown, L., (2014), Texture Shading: A New Technique for Depicting Terrain Relief. 9th ICA
769 Mountain Cartography Workshop, Banff, Canada.
- 770 Carena S., Suppe J., & Kao, H., (2004), Lack of Continuity of the San Andreas Fault in southern
771 California: 3-D fault models and earthquake scenarios. *Journal of Geophysical Research:*
772 *Solid Earth*, 109, B04313, doi:10.1029/2003JB002643

- 773 Çetin, H., Güneyli, H., & Mayer, L., (2003), Paleoseismology of the Palu-Lake Hazar Segment
 774 of the East Anatolian Fault Zone, Turkey. *Tectonophysics*, 374, 163–197.
 775 doi:10.1016/j.tecto.2003.08.003
- 776 Çetin, K. O., Ilgac, M., Can, G., Çakır, E., & Söylemez, B., (2020), January 24, 2020 Elazığ-
 777 Sivrice earthquake ($M_w=6.8$) reconnaissance study report (METU/EERC 2020-01):
 778 Middle East Technical University.
- 779 Daëron, M., Klinger, Y., Tapponnier, P., Elias, A., Jacques, E. & Sursock, A., (2007), 12,000-
 780 year-long record of 10 to 13 paleo-earthquakes on the Yammouneh fault, Levant fault
 781 system, Lebanon. *Bulletin of the Seismological Society of America*, 97(3), 749–771. doi:
 782 10.1785/0120060106
- 783 Darawcheh, R., Abdul-Wahed, M.K., & Hasan, A., (2022), The Great 1822 Aleppo Earthquake:
 784 New Historical Sources and Strong Ground Motion Simulation. *Geofisica Internacional*,
 785 61(3), 201–228.
- 786 Duman, T.Y., & Emre, Ö., (2013), The East Anatolian Fault: geometry, segmentation and jog
 787 characteristics. In A. H. F. Robertson, O. Parlak, & U. C. Ünlügenç (Eds.), *Geological*
 788 *Development of Anatolia and the Easternmost Mediterranean Region. Geological*
 789 *Society, London, Special Publications*, 372, <http://dx.doi.org/10.1144/SP372.14>
- 790 European Space Agency, Sinergise (2021). Copernicus Global Digital Elevation Model.
 791 <https://doi.org/10.5270/ESA-c5d3d65>. Accessed: 2023-02-12
- 792 ForM@Ter – EOST, (2023), Terrain displacement from the Türkiye-Syria earthquakes of
 793 February 6, 2023 obtained with the GDM-OPT-ETQ service applied on Sentinel-2 optical
 794 imagery. doi:10.25577/EWT8-KY06
- 795 Friedrich, A. M., Wernicke, B. P., Niemi, N. A., Bennett, R. A., & Davis, J. L., (2003),
 796 Comparison of geodetic and geologic data from the Wasatch region, Utah, and
 797 implications for the spectral character of Earth deformation at periods of 10 to 10 million
 798 years. *Journal of Geophysical Research: Solid Earth*, 108(B4), 2199,
 799 doi:10.1029/2001JB000682
- 800 Gasperini, P., & Ferrari, G., (2000), Deriving numerical estimates from descriptive information:
 801 The computation of earthquake parameters. *Annali di Geofisica*, 43(4), 729–746.
 802 DOI: 10.4401/ag-3670

- 803 Guidoboni, E., & Comastri, A., 2005. Catalogue of earthquakes and tsunamis in the
804 Mediterranean area from the 11th to the 15th century. INGV-SGA, Bologna, 1037 pp.
- 805 Guidoboni, E., Bernardini, F., & Comastri, A., (2004a), The 1138–1139 and 1156–1159
806 destructive seismic crises in Syria, south-eastern Turkey and northern Lebanon. *Journal*
807 *of Seismology*, 8, 105–127. <https://doi.org/10.1023/B:JOSE.0000009502.58351.06>
- 808 Guidoboni, E., Bernardini, F., Comastri, A., & Boschi, E., (2004b), The large earthquake on 29
809 June 1170 (Syria, Lebanon, and central southern Turkey). *Journal of Geophysical*
810 *Research: Solid Earth*, 109, B07304, doi:10.1029/2003JB002523
- 811 Guidoboni E., Ferrari G., Mariotti D., Comastri A., Tarabusi G., Sgattoni G., et al., (2018),
812 CFTI5Med, Catalogo dei Forti Terremoti in Italia (461 a.C.-1997) e nell'area
813 Mediterranea (760 a.C.-1500). Istituto Nazionale di Geofisica e Vulcanologia (INGV).
814 doi: <https://doi.org/10.6092/ingv.it-cfti5>
- 815 Guidoboni E., Ferrari G., Tarabusi G., Sgattoni G., Comastri A., Mariotti D., et al., (2019),
816 CFTI5Med, the new release of the catalogue of strong earthquakes in Italy and in the
817 Mediterranean area, *Scientific Data* 6, Article number: 80 (2019). doi:
818 <https://doi.org/10.1038/s41597-019-0091-9>
- 819 Gülerce, Z., Tanvir Shah, S., Menekşe, A., Arda Özacar, A., Kaymakci, N., & Önder Çetin, K.
820 (2017), Probabilistic seismic-hazard assessment for East Anatolian fault zone using
821 planar fault source models. *Bulletin of the Seismological Society of America*, 107(5),
822 2353-2366. <https://doi.org/10.1785/0120170009>
- 823 Gürboğa, S., and Gökçe, O., (2019), Paleoseismological catalog of Pre-2012 trench studies on
824 the active faults in Turkey. *Bulletin of Mineral Research and Exploration*, 159, 63–87.
825 <http://dx.doi.org/10.19111/bulletinofmre.561925>
- 826 Güvercin, S. E., Karabulut, H., Konca, A. Ö., Doğan, U., & Ergintav, S., (2022), Active
827 seismotectonics of the East Anatolian Fault. *Geophysical Journal International*, 230(1),
828 50–69. <https://doi.org/10.1093/gji/ggac045>
- 829 Hubert-Ferrari, A., Barka, A., Jacques, E., Nalbant, S. S., Meyer, B., Armijo, R., et al. (2000),
830 Seismic hazard in the Marmara Sea region following the 17 August 1999 Izmit
831 earthquake. *Nature*, 404, 269–273. <https://doi.org/10.1038/35005054>
- 832 Hubert-Ferrari, A., King, G., Manighetti, I., Armijo, R., Meyer, B., & Tapponnier, P., (2003),
833 Long-term elasticity in the continental lithosphere; modelling the Aden Ridge

- 834 propagation and the Anatolian extrusion process. *Geophysical Journal International*, 153,
835 111–132. <https://doi.org/10.1046/j.1365-246X.2003.01872.x>
- 836 Hubert-Ferrari, A., Lamair, L., Hage, S., Schmidt, S., Çağatay, M.N., & Avsar, U., (2020), A
837 3800 yr paleoseismic record (Lake Hazar sediments, eastern Turkey): Implications for the
838 East Anatolian Fault seismic cycle. *Earth and Planetary Science Letters*, 538, 11615.
839 <https://doi.org/10.1016/j.epsl.2020.116152>
- 840 Karakhanian, A. S., Trifonov, V. G., Ivanova, T. P., Avagyan, A., Rukieh, M., Minini, H., et al.,
841 (2008), Seismic deformation in the St. Simeon Monasteries (Qal'at Sim'an), Northwestern
842 Syria. *Tectonophysics*, 453, 122–147. doi:10.1016/j.tecto.2007.03.008
- 843 Khair, K., Karakaisis, G. F., & Papadimitriou, E., (2000), Seismic zonation of the Dead Sea
844 transform fault area. *Annali di Geofisica*, 43(1), 61–79. DOI: 10.4401/ag-3620
- 845 King, G. C. P., Stein, R. S. & Lin, J., (1994), Static stress changes and the triggering of
846 earthquakes. *Bulletin of the Seismological Society of America*, 84, 935–953.
847 <https://doi.org/10.1785/BSSA0840030935>
- 848 Kondorskaya, R. N. V. & Ulomov, V. I., (1999), Special Catalogue of Earthquakes of Northern
849 Eurasia (SECNE) from Ancient Times through 1995. Joint Institute of Physics of the
850 Earth (JIPE), Russian Academy of Sciences, Moscow.
- 851 Lefevre, M., Klinger, Y., Al-Qaryouti, M., Le Béon, M., & Moumani, K., (2018), Slip deficit
852 and temporal clustering along the Dead Sea fault from paleoseismological investigations.
853 *Scientific reports*, 8(1), 4511. <https://doi.org/10.1038/s41598-018-22627-9>
- 854 Marco, S., & Klinger, Y., (2014), Review of on-fault palaeoseismic studies along the Dead Sea
855 Fault. *Dead Sea transform fault system: Reviews*, 183–205. DOI: 10.1007/978-94-017-
856 8872-4_7
- 857 McCaffrey, R., (2008), Global frequency of magnitude 9 earthquakes. *Geology*, 36(3), 263–266.
858 doi: 10.1130/G24402A.1
- 859 Meghraoui, M., Gomez, F., Sbeinati, R., Van der Woerd, J., Mouty, M., Darkal, A. N., et al.,
860 (2003), Evidence for 830 years of seismic quiescence from palaeoseismology,
861 archaeoseismology and historical seismicity along the Dead Sea fault in Syria. *Earth and*
862 *Planetary Science Letters*, 210, 35–52. [https://doi.org/10.1016/S0012-821X\(03\)00144-4](https://doi.org/10.1016/S0012-821X(03)00144-4)
- 863 Ou, Q., Lazecky, M., Watson, C.S., Maghsoudi, Y., & Wright, T., (2023), 3D Displacements and
864 Strain from the 2023 February Turkey Earthquakes, version 1. NERC EDS Centre for

- 865 Environmental Data Analysis, *14 March 2023*.
 866 <https://dx.doi.org/10.5285/df93e92a3adc46b9a5c4bd3a547cd242>
- 867 Öztürk, S., (2021), Spatio-temporal Analysis on the Aftershocks of January 24, 2020, M_w 6.8
 868 Sivrice- Elazığ (Turkey) Earthquake. PACE-2021 International Congress on the
 869 Phenomenological Aspects of Civil Engineering, 20-23 June 2021, Atatürk University,
 870 Erzurum, paper 364.
- 871 Papathanassiou, G., Pavlides, S., Christaras, B., & Pitolakis, K., (2005), Liquefaction case
 872 histories and empirical relations of earthquake magnitude versus distance from the
 873 broader Aegean region. *Journal of Geodynamics*, *40*(2–3), 257–78.
 874 <https://doi.org/10.1016/j.jog.2005.07.007>
- 875 Perinçek, D., & Çemen, I., (1990), The structural relationship between the East Anatolian and
 876 Dead Sea fault zones in southeastern Turkey. *Tectonophysics*, *172*, 331–340.
 877 [https://doi.org/10.1016/0040-1951\(90\)90039-B](https://doi.org/10.1016/0040-1951(90)90039-B)
- 878 Philibosian, B., & Meltzner, A. J., (2020), Segmentation and supercycles: A catalog of
 879 earthquake rupture patterns from the Sumatran Sunda Megathrust and other well-studied
 880 faults worldwide. *Quaternary Science Reviews*, *241*, 106390.
 881 <https://doi.org/10.1016/j.quascirev.2020.106390>
- 882 Pousse-Beltran, L., Nissen, E., Bergman, E. A., Cambaz, M. D., Gaudreau, É., Karasözen, E., et
 883 al., (2020), The 2020 M_w 6.8 Elazığ (Turkey) earthquake reveals rupture behavior of the
 884 East Anatolian Fault. *Geophysical Research Letters*, *47*, e2020GL088136.
 885 <https://doi.org/10.1029/2020GL088136>
- 886 Reitman, N. G., Briggs, R. W., Barnhart, W. D., Thompson Jobe, J. A., DuRoss, C. B., Hatem,
 887 A. E., et al., (2023), Preliminary fault rupture mapping of the 2023 M_w 7.8 Türkiye
 888 Earthquakes. <https://doi.org/10.5066/P985I7U2>
- 889 Rosakis, A., Abdelmeguid, M., & Elbanna, A., (2023), Evidence of Early Supershear Transition
 890 in the M_w 7.8 Kahramanmaraş Earthquake From Near-Field Records. *EarthArXiv*
 891 [preprint] <https://doi.org/10.31223/X5W95G>, 17 February 2023.
- 892 Rukieh, M., Trifonov, V. G., Dodonov, A. E., Minini, H., Ammar, O., Ivanov, T. P., et al.,
 893 (2005), Neotectonic map of Syria and some aspects of Late Cenozoic evolution of the
 894 northwestern boundary zone of the Arabian plate. *Journal of Geodynamics*, *40*, 235–256.
 895 [doi:10.1016/j.jog.2005.07.016](https://doi.org/10.1016/j.jog.2005.07.016)

- 896 Salamon, A., (2008), Patterns of aftershock sequences along the Dead Sea Transform -
897 Interpretation of historical seismicity. *Geological Survey of Israel, Report GSI/05/2008*,
898 78 pp.
- 899 Salditch, L., Stein, S., Neely, J., Spencer, B.D., Brooks, E.M., Agnon, A., et al., (2020),
900 Earthquake supercycles and long-term fault memory. *Tectonophysics*, 774, 228289.
901 <https://doi.org/10.1016/j.tecto.2019.228289>
- 902 Satılmış, S., (2016), 1893 Malatya Earthquake and Disaster Management. *Journal Of The Center*
903 *For Ottoman Studies Ankara University*, 39, 137-177.
- 904 Sbeinati, M. R., Darawcheh, R. & Mouty, M., (2005), The historical earthquakes of Syria: an
905 analysis of large and moderate earthquakes from 1365 B.C. to 1900 A.D. *Annals of*
906 *Geophysics*, 47, 733-758.
- 907 Sbeinati, M. R., Meghraoui, M., Suleyman, G., Gomez, F., Grootes, P., Nadeau, et al., (2010),
908 Timing of earthquake ruptures at the Al Harif Roman aqueduct (Dead Sea fault, Syria)
909 from archaeoseismology and paleoseismology. In M. Sintubin, I. S. Stewart, T. M.
910 Niemi, & E. Altunel (Eds.), *Ancient Earthquakes: Geological Society of America Special*
911 *Paper 471*, p. 243–267, doi: 10.1130/2010.2471(20)
- 912 Seyrek, A., Demir, T., Pringle, M.S., Yurtmen, S., Westaway, R.W.C., Beck, A., et al., (2007),
913 Kinematics of the Amanos Fault, southern Turkey, from Ar/Ar dating of offset
914 Pleistocene basalt flows: transpression between the African and Arabian plates. In W. D.
915 Cunningham, & P. Mann (Eds), *Tectonics of Strike-Slip Restraining and Releasing*
916 *Bends. Geological Society, London, Special Publications*, 290, 255–284. DOI:
917 10.1144/SP290.9
- 918 Seyrek, A., Demir, T., Westaway, R., Guillou, H., Scaillet, S., White, T. S., et al., (2014), The
919 kinematics of central-southern Turkey and northwest Syria revisited. *Tectonophysics*,
920 618, 35–66. <http://dx.doi.org/10.1016/j.tecto.2014.01.008>
- 921 Stein, R. S., Barka, A. A., & Dieterich, J. H., (1997), Progressive failure on the North Anatolian
922 fault since 1939 by earthquake stress triggering. *Geophysical Journal International*,
923 128(3), 594–604. <https://doi.org/10.1111/j.1365-246X.1997.tb05321.x>
- 924 Taftoglou, M., Valkaniotis, S., Karantanellis, E., Goula, E., & Papathanassiou, G., (2023),
925 Preliminary mapping of liquefaction phenomena triggered by the February 6 2023 M7.7

- 926 earthquake, Türkiye / Syria, based on remote sensing data. Zenodo,
 927 doi:10.5281/zenodo.7668400
- 928 Tozer, B., Sandwell, D. T., Smith, W. H. F., Olson, C., Beale, J. R., & Wessel, P., (2019), Global
 929 Bathymetry and Topography at 15 Arc Sec: SRTM15+. *Earth and Space Science*, 6(10),
 930 1847–1864. <https://doi.org/10.1029/2019EA000658>
- 931 U.S. Geological Survey, (2023), Earthquake Lists, Maps, and Statistics. Accessed March 26,
 932 2023 at URL [https://www.usgs.gov/natural-hazards/earthquake-hazards/lists-maps-and-](https://www.usgs.gov/natural-hazards/earthquake-hazards/lists-maps-and-statistics)
 933 [statistics](https://www.usgs.gov/natural-hazards/earthquake-hazards/lists-maps-and-statistics)
- 934 Wan, Y., Shen, Z.-K., Bürgmann, R., Sun, J., & Wang, M., (2017), Fault geometry and slip
 935 distribution of the 2008 M_w 7.9 Wenchuan, China earthquake, inferred from GPS and
 936 InSAR measurements. *Geophysical Journal International*, 208, 748-766. doi:
 937 10.1093/gji/ggw421
- 938 Wells, D. L., & Coppersmith, K. J., (1994), New empirical relationships among magnitude,
 939 rupture length, rupture width, rupture area, and surface displacement. *Bulletin of the*
 940 *Seismological Society of America*, 84(4), 974 – 1002.
 941 <https://doi.org/10.1785/BSSA0840040974>
- 942 Wessel, P., Luis, J. F., Uieda, L., Scharroo, R., Wobbe, F., Smith, W. H. F., et al., (2019), The
 943 Generic Mapping Tools version 6. *Geochemistry, Geophysics, Geosystems*, 20, 5556–
 944 5564. <https://doi.org/10.1029/2019GC008515>
- 945 Westaway, R., (2004), Kinematic consistency between the Dead Sea Fault Zone and the
 946 Neogene and Quaternary left-lateral faulting in SE Turkey. *Tectonophysics*, 391(1-4),
 947 203-237. <https://doi.org/10.1016/j.tecto.2004.07.014>
- 948 Yönlü, Ö., (2012), Late Quaternary Activity of The East Anatolian Fault Zone Between Gölbaşı
 949 (Adıyaman) And Karataş (Adana). Doctoral dissertation, Dept. of Geological
 950 Engineering, Eskişehir Osmangazi Üniversitesi, June 2012 (in Turkish).
- 951 Zelenin, E., Bachmanov, D., Garipova, S., Trifonov, V., & Kozhurin, A., (2022), The Active
 952 Faults of Eurasia Database (AFEAD): the ontology and design behind the continental-
 953 scale dataset. *Earth System Science Data*, 14, 4489-4503. [https://doi.org/10.5194/essd-](https://doi.org/10.5194/essd-14-4489-2022)
 954 [14-4489–2022](https://doi.org/10.5194/essd-14-4489-2022)
- 955

956 **Table 1.** List of earthquakes and corresponding source faults.

Date ^a	M _w ^b	Name ^a	Rupture length (km) ^b	Aftershocks (months)	Source fault or fault segment
Feb. 06, 2023	7.8	Pazarcık	~ 310	ongoing	Amanos, Pazarcık, & Erkenek s.
Jan. 24, 2020	6.8	Elâziğ	(~ 35)	19 ^c	Pütürge s.
Mar. 02, 1893	7.2 +/- 0.1	Malatya	~ 60	> 12 ^d	Erkenek s.
Jan. 14, 1874	7.1	Sarikamiş	~ 45	≥ 12 ^f	Palu s.
Apr. 03, 1872	7.2	Amik Gölü	~ 50	10 ^c	Kirikhan s. & Antakya f. z.
Aug. 13, 1822	7.5	Southeastern Anatolia	~ 110	30 ^c	Yesemek f. & Qanaya-Babatorun f.
Jan. 21, 1626	7.2	Hama	~ 50	unknown	northern St. Simeon f.
1513/1514	≥ 7.4	Malatya	≥ 80	unknown	Pazarcık & Nurdağı s.
Dec. 29, 1408	7.0	Shugr-Bekas	~ 40	unknown	Qanaya-Babatorun f.
Feb. 20, 1404	≥ 7.0	Aleppo	≥ 40	≥ 9 ^{f,g}	Nusayriyah f.
Jun. 29, 1170	7.3 – 7.4	Shaizar	~ 80	4 ^c	Missyaf f.
Aug. 12, 1157	7.2	Apamea	~ 50	21 ^c	Shaizar f.
Oct. 11, 1138	7.2	Atharib	~ 50	8 ^c	northern St. Simeon f.
Nov. 29, 1114	≥ 7.2	Antioch, Maraş	≥ 50	5 ^f	Pazarcık s.

957

958 ^aAmbraseys (2009), except for events from 2020 (Çetin et al. 2020) and 2023 (U.S. Geological
959 Survey, 2023).

960 ^b For most of the earthquakes we have estimated surface rupture lengths based on Wells &
961 Coppersmith (1994), unless lengths were reported in original sources (discussion in text). The
962 magnitude reported here is our preferred one among the sources discussed in the text. For the
963 Elâziğ earthquake the rupture length value is in brackets because it did not rupture at the surface,
964 though it had shallow slip (Pousse-Beltran et al., 2020).

965 ^c Salamon, 2008; ^dSatılmış, 2016; ^eÖztürk, 2021; ^fAmbraseys, 2009

966 ^g not possible to really distinguish all aftershocks of 1404 from foreshocks of 1408.

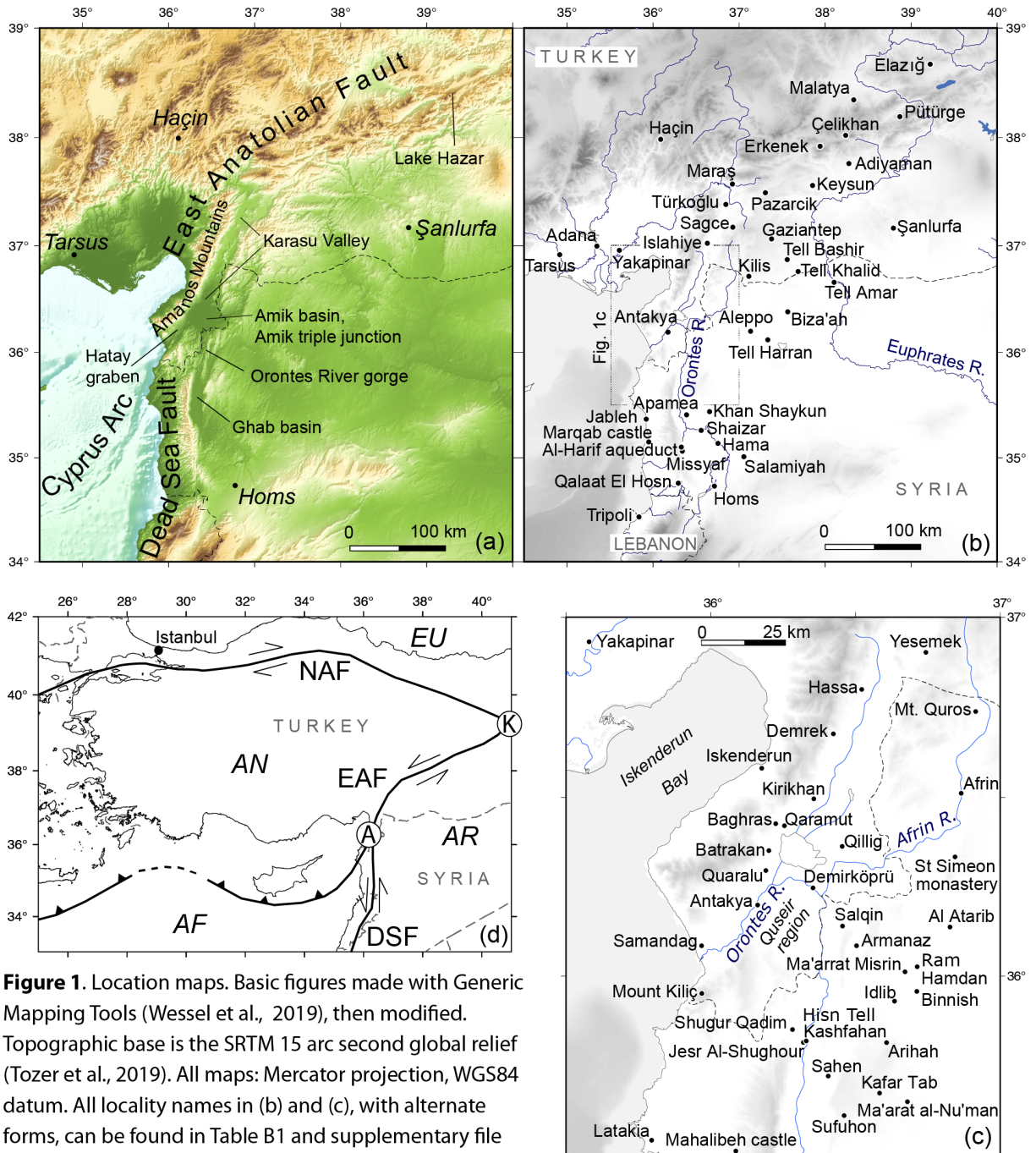


Figure 1. Location maps. Basic figures made with Generic Mapping Tools (Wessel et al., 2019), then modified. Topographic base is the SRTM 15 arc second global relief (Tozer et al., 2019). All maps: Mercator projection, WGS84 datum. All locality names in (b) and (c), with alternate forms, can be found in Table B1 and supplementary file ds04. NAF = North Anatolian Fault, EAF = East Anatolian Fault, DSF = Dead Sea Fault, K = Karloiova triple junction, A = Amik triple junction; AF = African plate, AN = Anatolian plate, AR = Arabian plate, EU = Eurasian plate.

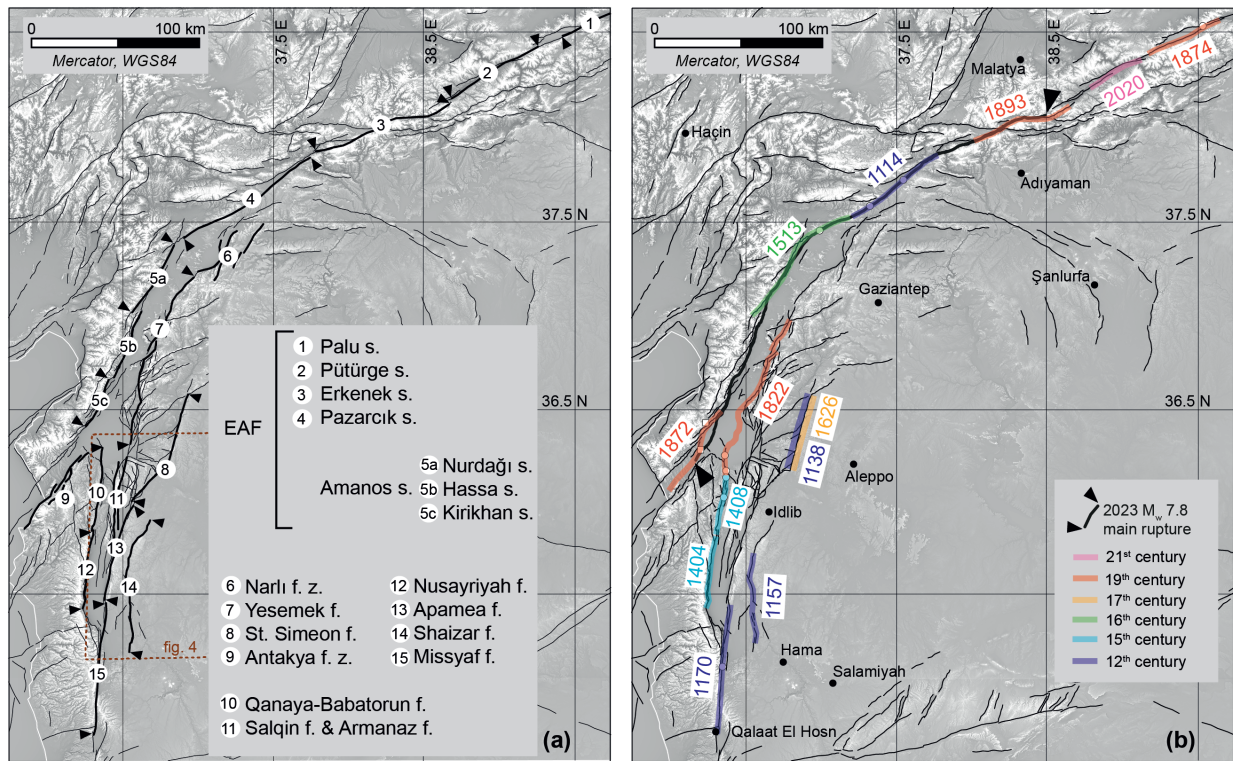


Figure 2. (a) Fault names (see Appendix B for details). The Amanos segment of the EAF is split into three further segments. Bends and stepovers are not labeled here because we do not refer to them; their names can be found in Duman & Emre (2013). s. = segment, f. = fault, f. z. = fault zone. (b) Fault rupture/earthquake pairs from Table 1. Base map and other elements are described and referenced in figure 3. Original uninterpreted base map included as supplementary file ds01, and ruptures as supplementary file ds03.

968

969

970

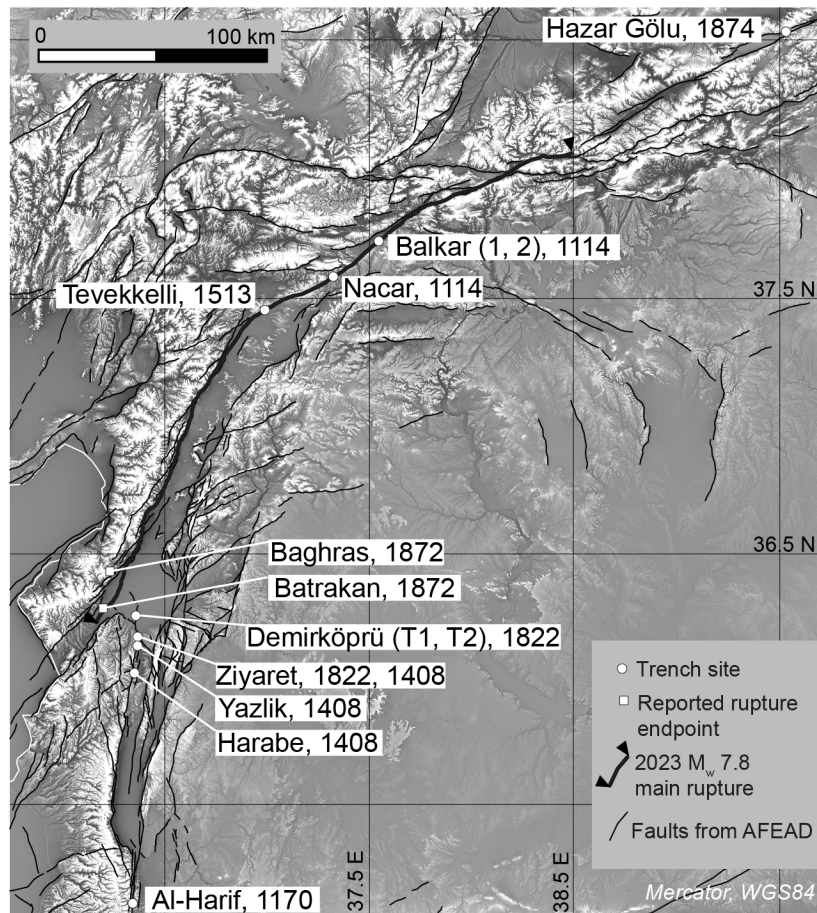


Figure 3. Location and names of trenches, and approximate historical fault rupture endpoints mentioned in the text, with the relevant pre-2023 earthquake/s indicated for each one. See references in text for each trench name. AFEAD faults are from Zelenin et al. (2022), whereas the 2023 main rupture we remapped ourselves from the pixel tracking data of Ou et al. (2023) and ForMTMTer - EOST (2023), and from the preliminary maps of Reitman et al. (2023). Basemap derived from the 30 m GLO-30 Copernicus DEM (European Space Agency, 2021), processed by applying the texture shading technique of Brown (2014).

971

972

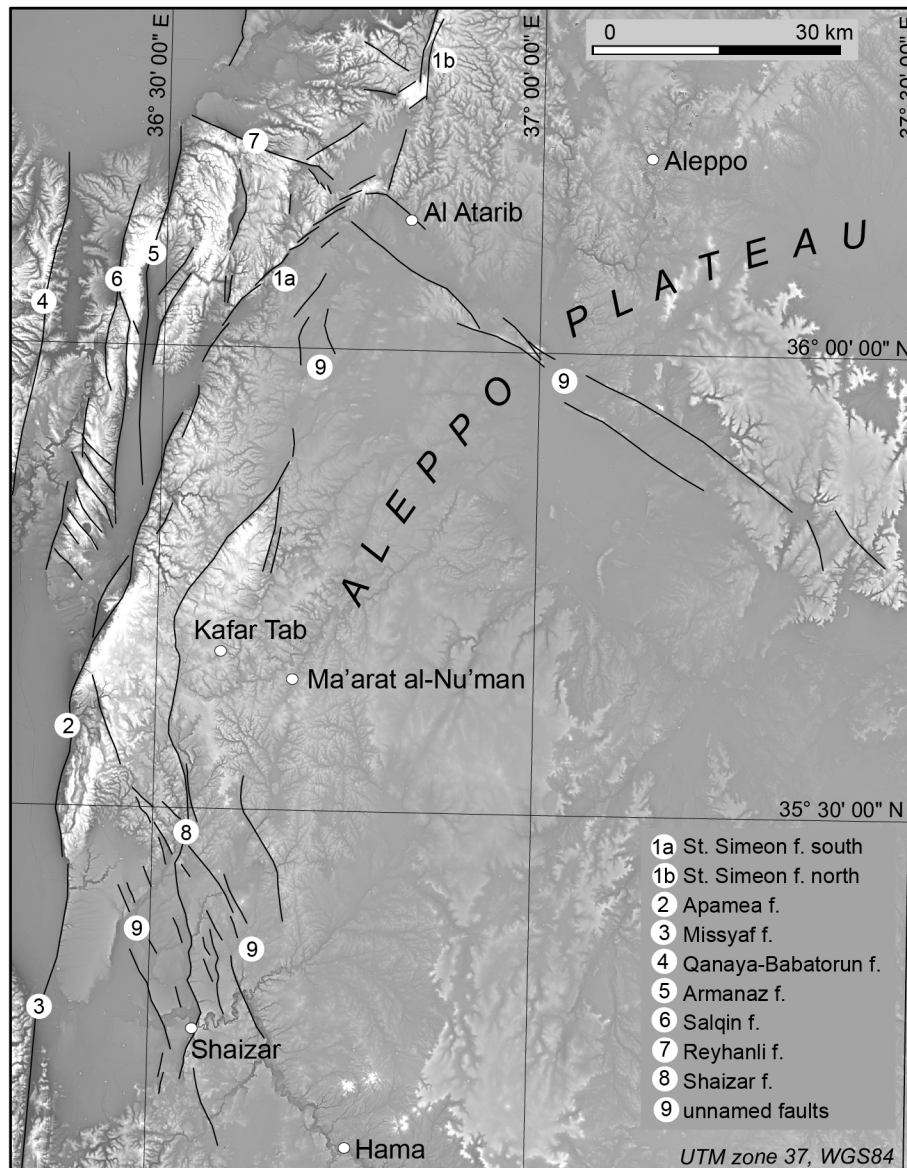


Figure 4. Faults that we mapped using the 30 m GLO-30 Copernicus DEM (European Space Agency, 2021) processed by applying the texture shading technique of Brown (2014), which can be used to enhance fine details (e.g. scarps). We mapped only the very sharpest features, which are likely to be active faults, but there are also numerous other more subtle lineaments. The background image has been muted for clarity; a full-strength and full-resolution uninterpreted image is included as a supplement (file ds02).

973

974

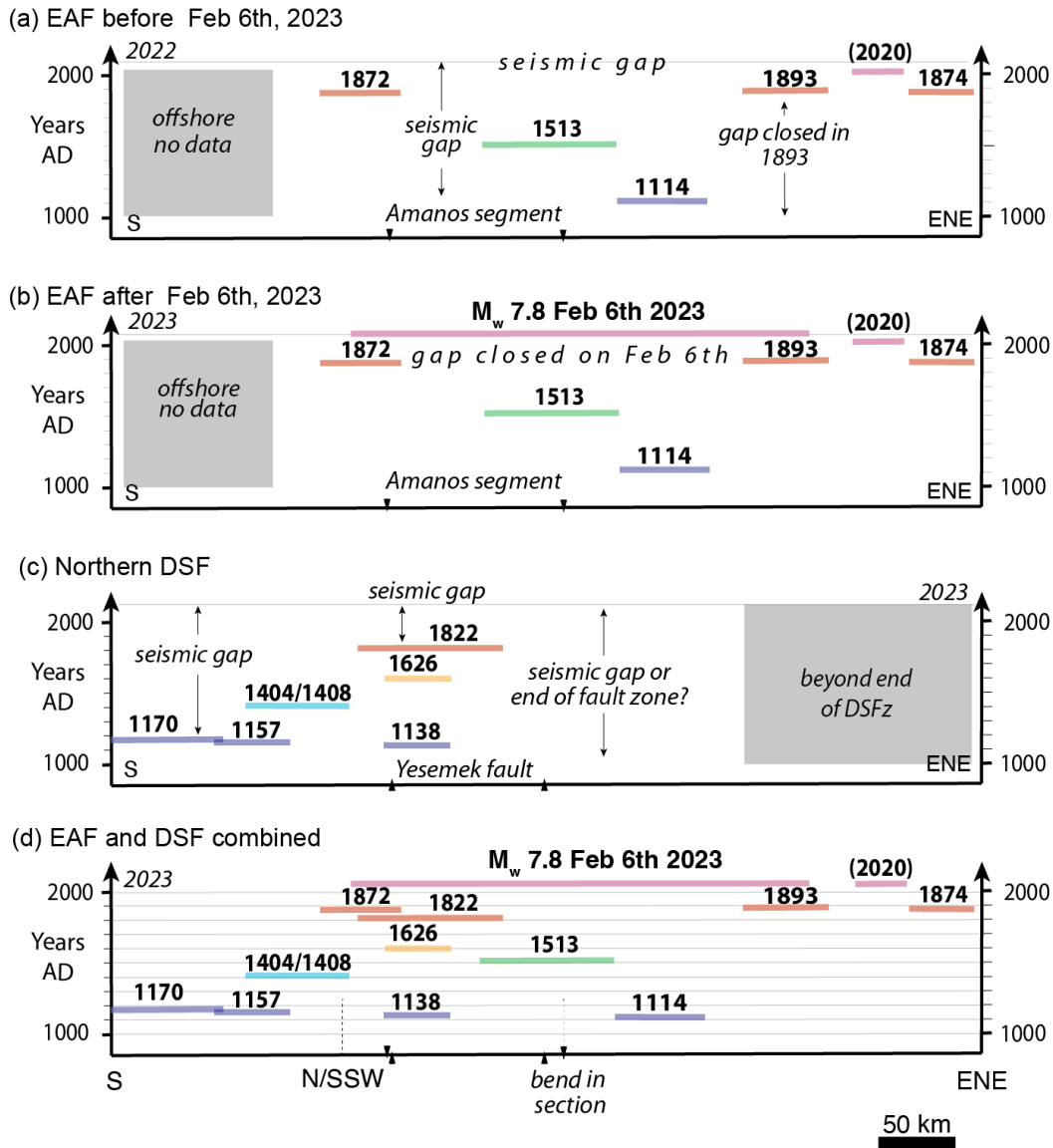


Figure 5. Space-time pattern of historic earthquakes along the EAF and northern DSF (see Figure 2 for location). The position and extent of $M > 7$ ruptures (horizontal bars) are justified in the text. (a and b) Pattern of $M > 7$ ruptures for the western portion of the EAF prior to and after February 6th, 2023. (c) Pattern of $M > 7$ ruptures for the northern DSF. (d) Pattern of all recorded $M > 7$ ruptures for the region in which both active strike-slip fault systems (EAF and DSF) overlap spatially and interact kinematically.

976 **Appendix A: earthquake magnitudes**

977 For earthquake magnitudes between 6.2 and 8.2 and depth of focus < 70 km, $M_w = M_s$
 978 (Scordilis, 2006). As we only consider events in this magnitude range and discuss a few
 979 instrumental events for which M_w is reported, we always use M_w in our text unless it is necessary
 980 to specifically mention another type of magnitude, with the understanding that, when citing
 981 historical sources, these mostly reported either M_s determined using local empirical relationships
 982 based on rupture length, or M_F (“felt magnitude” equivalent to M_s , see below) (e.g. Ambraseys,
 983 1988; Ambraseys & Barazangi, 1989). Another magnitude used by the INGV CIFT5Med catalog
 984 (Guidoboni et al., 2018, 2019) is M_e , which here stands for “magnitude equivalent” (i.e.
 985 equivalent to M_w) as calculated from intensities (whereas usually M_e stands for “energy
 986 magnitude” calculated from energy release) which, as far as uncertainties are concerned, we treat
 987 as M_F , because it is also fundamentally based on reported intensity areas. The difference between
 988 M_e and M_F appears to be simply the specific relationship between intensity and magnitude used,
 989 which for M_e is the one of Gasperini and Ferrari (2000). Considering that the largest source of
 990 uncertainty in estimating magnitude is the interpretation of the historical descriptions themselves,
 991 which determine what intensity is assigned to each place (for example, where one author assigns
 992 intensity X, another may assign intensity VIII), the specific relationship used does not seem to be
 993 overly important, as long as it is properly calibrated for local conditions.

994 To better understand this source of uncertainty, we have recalculated magnitudes
 995 ourselves for all the historical earthquakes that we considered whenever sufficient information
 996 was available, using the M_F relationship developed for Turkey by Ambraseys & Finkel (1987)
 997 and re-interpreting assigned intensities from descriptions, if necessary (especially in cases of
 998 conflicting opinions), before deciding which reported magnitude to adopt in our work:

$$999 \quad M_F = -0.53 + 0.58(I_i) + 1.96 \times 10^{-3}(R_i) + 1.83 \log(R_i),$$

1000 where R_i is the average radius (in km) of the isoseismal of intensity I_i

1001 The reason we used M_F in our own tests instead of M_s is because not all events have a
 1002 reported rupture length (which, even when reported, may be underestimated, as discussed by
 1003 Ambraseys & Jackson, 1998), but nearly all have at least a “felt area”. From comparing previous
 1004 authors’ works in this region with our own test results, the uncertainty in magnitude estimated
 1005 for historical earthquakes of +/- 0.3 (Ambraseys, 1989) seems to be about right (Table A1).

1006 The addition of the 2023 events allowed us also to verify that this empirical relationship
1007 is indeed appropriate for the region, as the M_F we calculated for the two events using intensity
1008 maps from U.S. Geological Survey (2023) are $7.7 +0.2/-0.1$ and $7.3 +/-0.2$ respectively (Table
1009 A1). Considering that different seismological laboratories in the US and Turkey (USGS, GCMT,
1010 GEOSCOPE, KOERI) have variably reported M_w of 7.7, 7.8, and 8.0 for the first event, and 7.5,
1011 7.6, and 7.7 for the second, our estimate of M_F is well within range and validates the use of this
1012 formula for older earthquakes in the region, with $+/- 0.3$ also a reasonable, conservative
1013 uncertainty.

1014

1015 **Table A1.** List of earthquakes with M_F recalculated by us, and all magnitudes reported by
 1016 previous authors^a.

Date^b	M_F	Reported magnitude^a	Name^b
Feb. 06, 2023	7.3 +/- 0.2	M_w 7.5, 7.6, 7.7	Elbistan
Feb. 06, 2023	7.7 +0.2/-0.1	M_w 7.7, 7.8, 8.0	Pazarcık
Jan. 24, 2020	6.6	M_w 6.7, 6.8	Elâziğ
Mar. 02, 1893	7.0	≥ 7.1 ; 7.2 +/- 0.1	Malatya
Jan. 14, 1874	7.0 +/- 0.1	≥ 7.1	Sarikamiş
Apr. 03, 1872	7.1 +0.2/-0.1	5.9 ^c ; ≤ 7.2 ; 7.2	Amik Gölü
Aug. 13, 1822	7.5 +0.3/-0.2	7.0; ≥ 7.4 ; 7.5	Southeastern Anatolia
Jan. 21, 1626	-	7.2	Hama
1513/1514	$\geq 7.4^d$	≥ 7.4	Malatya
Dec. 29, 1408	7.1 +/- 0.1	7.0; 6 to 7; 7.4	Shugr-Bekas
Feb. 20, 1404	7.4	≥ 7.0 ; 7.4	Aleppo
Jun. 29, 1170	7.3 +0.2/-0.4	7.3 – 7.4; 7.3+/- 0.3; 7 to 7.8; 7.7	Shaizar
Aug. 12, 1157	7.4 +/- 0.1	7.2 +/- 0.3; 7.4	Apamea
Oct. 11, 1138	7.1 +/- 0.5	6.0; 7.5	Atharib
Nov. 29, 1114	7.3 +/- 0.4	6.9 +/- 0.3; ≥ 7.2 ; 7.4; ≥ 7.8	Antioch, Maraş

1017
 1018 ^a Unless M_w is explicitly indicated, the reported magnitude is either M_s , M_F , or M_e as explained
 1019 in the text.

1020 ^b Ambraseys (2009) except for 2020 (Çetin et al., 2020) and 2023 events (U.S. Geological
 1021 Survey, 2023).

1022 ^c Sbeinati et al. (2005). It is unclear where they get this low value from, because it is very
 1023 different from those of the authors they cite, and it seems to conflict with the size of the high
 1024 damage area and the highest reported intensity when compared to the other events they have in
 1025 the same catalog.

1026 ^d Due to the limited information, only one intensity area can be defined, so the magnitude
 1027 depends on whether this intensity is assigned as VI or VII (because significant “destruction” was
 1028 reported in all localities mentioned, it should be at least VI, i.e. strong shaking).

1029

1030

1031 Appendix B: fault names and place names

1032 There seems to be no generally accepted standard about names of faults and fault
1033 segments in the region. One problem is the political border between Turkey and Syria: as it
1034 happens too often, faults (and their names) have a tendency to end or change at the border. The
1035 Active Faults of Eurasia Database (AFEAD) of Zelenin et al. (2022) often does not label the
1036 individual fault segments beyond naming the general fault zone to which they belong. For the
1037 East Anatolian fault system, we have decided to use the segment names and segment boundaries
1038 as defined in Duman & Emre (2013), because these authors go through the effort of
1039 systematically providing detailed maps, coordinates, and names in a way that is easy to follow.
1040 In the case of faults that are traditionally considered part of the Dead Sea fault system, the choice
1041 is less straightforward, because even when a fault has been labeled, its endpoints are usually ill-
1042 defined, or a vague description (e.g. “fault on the eastern side of the Ghab basin”) is given, and
1043 maps in publications are small and hard to read. We chose to use the labeling of Westaway
1044 (2004) and Seyrek et al. (2012) for the following faults: Qanaya-Babatorun (called instead
1045 “Hacıpaşa segment” to the Syrian border by Akyüz et al., 2006), Nusayriyah, Apamea, Salqin,
1046 and Armanaz, which are named after nearby towns and villages. These authors also define a
1047 “East Hatay fault” on the eastern edge of the Karasu graben, whereas the same fault is called
1048 “Yesemek fault” by Duman & Emre (2013). We chose to keep the latter name because it has
1049 been assigned based on the fault going through the village of Yesemek, whereas “East Hatay”
1050 refers to a region. Finally, different authors assign the name “Afrin” (or Aafrin) fault to two
1051 entirely different faults that pass near the town of Afrin. One of these two does not appear in our
1052 analysis, but to avoid any confusion, we have decided to call the fault that we discuss “St.
1053 Simeon fault” as named by Rukieh et al. (2005) and Karakhanian et al. (2008) due to the fault
1054 passing through the St. Simeon monastery site (whereas Westaway, 2004, and Seyrek et al.,
1055 2012, call this “Afrin fault”). We were not able to find any existing names for the faults east of
1056 Apamea in Syria (on the Aleppo plateau, between the Ghab basin and Aleppo, see Figure 4), so
1057 to avoid using the “unnamed” label more than necessary, we named the largest of these “Shaizar
1058 fault”, because it goes through the town bearing this name, which was destroyed in the 1157
1059 earthquake.

1060 Place names in this region have changed throughout the centuries depending on who
1061 controlled which territory, and even today the same name is spelled differently depending on

1062 transliteration and on native language of the writer. In reading the various publications and
1063 earthquake catalogs we had to go to some lengths to match place names from one publication to
1064 the next, and to modern-day names that anyone can find on Google Earth. Thus, besides the
1065 standard map with locations (Figure 1), we are also including a simplified table of place names
1066 in this appendix (Table B1), plus an electronic version of it that reports all the variants we have
1067 encountered (up to six), coordinates, and any comments where needed (Supplementary file
1068 ds04). The list is by no means exhaustive, but it should help readers find their way from one
1069 publication to the next. In our paper we have decided which name to use mostly based on the
1070 primary source of our information, except for those cases where a modern name was easier to
1071 find in online searches and the name appears many times in our text (e.g. Demirköprü instead of
1072 Jisr al-Hadid). In those cases where the modern locality name has nothing to do with the one in
1073 historical records (we just matched positions between the published map and Google Earth map
1074 to identify its coordinates), we have kept the historical name in our text and maps, but supplied
1075 the name of today's nearest locality in the table (e.g. Batrakan/Atatürk).

1076

1077 **Table B1.** Place names from Figure 1, listed alphabetically in first column: in bold is the version
 1078 used in text and figures. Full version in Supplementary file ds04.

1079
 1080
 1081
 1082
 1083

<i>Google Earth name</i>	<i>Alternate name 1</i>	<i>Alternate name 2</i>
Afamiyah	Apamea	Afamea
Afrin	Aafrine	Aafrin
Al Atarib	Al-Atareb	Cerepum
Alazi	Qaralu	
Aleppo	Halab	Halep
Antakya	Antioch	Hatay
Armanaz	Armenhaz	
Asmacık	Tell Khalid	Trihalet
Atatürk	Batrankan	
Bakras Kalesi	Baghras	Bagras
Biza'ah	Bizza	
Demirköprü	Jisr al-Hadid	Jisr El Hadid
Gaziantep	Aintab	Gaziaintab
Hama	Hamat	Hamath
Haram	Harim	Uringa
Homs	Hims	Emesa
Iskenderun	Alexandretta	Scanderoon
Jableh	Jeble	Jabala
Jesr Al-Shughour	Jisr al-Shughur	Jisr as-Shugr
karamurt Hani	Qaramut	
Khan Shaykhun	Han Sheikhun	
Kharamanmaraş	Maraş	Germanicea
Kozkalesi	Quseyr	Quseir
Kumlu	Qillig	Quilliq
Latakia	Al-Ladhiqiya	Laodicea
Ma'arat al-Nu'man	Marre	Arra
Ma'arrat Misrin	Ma'aret Masrin	Megaret Basrin
Mahalibeh castle	Qalaat Blatnes	Balatonus
Marqab castle	Markab	Margat
Missyaf	Masyaf	Misyaf
Mount Kiliç	Mount Cassius	Al-Akraa
Orontes / Asi	Arantu	
Qalaat El Hosn	Krak (Crak, or Crac) des Chevaliers	Hisn al-Akrad
Saimbeyli	Haçin	Kaza Haçin
Sakcagoz	Sagce	Sakçagözü
Salamiyah	Salamyya	Salamiyyah
Salqin	Salqein	
Samandag	Suaidiya	Seleucia
Şanlurfa	Urfa	Edessa
Serjilla	Kafar Tab	Capharda
Shaizar	Shayzar	
Shugur Qadim	Castles of Shughur and Bekas	Shugr-Bekas
Tell Arn	Tell Harran	Tal 'Aran
Tilbasar Kalesi	Tell Bashir	Turbessel
Tripoli	Tarabulus	
Yakapınar	Misis	Mopsuestia